An important recent study has established the magmatic O isotopic compositions of zircons in Ediacaran granitic rocks in Sinai. O isotopic compositions of granitic whole-rock samples are not reliable because hydrothermal and deuteric alteration is common, but O isotopic values determined from zircons are robust and preserve magmatic information because of the refractory character of zircon. Be'eri-Shlevin et al. (2009c) analyzed zircons from well dated granitic, post-collisional calc-alkaline (~635–590 Ma) and alkaline (~608–580 Ma) rocks from Sinai. Both suites have indistinguishable and restricted $\delta^{18}O$ values of 5.7 and 5.8‰, which points to dominance of mantle-like $\delta^{18}O$ sources in their formation, either because of anatexis in the lower crust or fractionation of mafic melts. Be'eri-Shlevin et al. (2009c) concluded that the granitic magmas were derived from mantle-like $\delta^{18}O$ reservoirs, with little evidence for involvement of altered juvenile crust, except in the northernmost Sinai basement.

With regard to trace-element geochemistry for late Cryogenian–Ediacaran granitoids in the ANS, data are not systematically available, but what are available show some differences in trace-element contents and REE patterns that help to distinguish between calc-alkaline I-type granitoids and A-type granitoids, although there is significant overlap and discrimination is not always clear. For example, most calc-alkaline ANS granitoids plot in the fields of volcanic-arc and syn-collisional granites on the Nb/Y and Rb/Y + Nb diagrams of Pearce et al. (1984), but many samples also plot in the post-collisional Rb/Y + Nb sub-field of Pearce (1996) and some extend into the within-plate field. Examples include the 630 Ma granitoids sampled by Teklay et al. (2001) in the Nakfa terrane in the southern part of the ANS, metaluminous and peraluminous CA2 granitoids as well as some CA1 granitoids studied by Be'eri-Shlevin et al. (2009b) in Sinai, and most granitoids in the Aqaba suite in Jordan (Jarrar et al., 2003). The Nakfa granitoids of Eritrea have slightly LREE-enriched REE patterns; some samples have negative Eu anomalies, others positive anomalies (Teklay et al., 2001). Calc-alkaline mafic and felsic plutons in Sinai show moderate REE enrichment and steep REE patterns, with no to slight Eu anomalies on chondrite-normalized REE plots (Be'eri-Shlevin et al., 2009b). Mafic members of the Aqaba suite (640–600 MA) in Jordan are enriched in LILE relative to HFSE and are moderately enriched in REE [$(La/Lu)n$ = 5–11], traits typical of arc basalts. Granitoids of the same suite are high in Ba, Sr, and LREE, have low Y and have steep REE patterns [$(La/Lu)n$ = 20–25]. They have low-initial $^{87}Sr/^{86}Sr$ (~0.70305) and high ε_{Nd} values (+2.3–5.0) and may have been generated by high degrees of partial melting (10–30%) of subducted oceanic crust, with or without a small proportion of ocean sediments (Jarrar et al., 2003).

Late Cryogenian–Ediacaran A-type granitoids in the North Eastern Desert (NED) (Moussa et al. (2008) include peraluminous granites that plot in the within-plate and post-collisional fields of Pearce et al. (1984) and Pearce (1996). Similar rocks in Sinai mostly plot as within-plate granites although some extend into the volcanic-arc field of Pearce et al. (1984) but are all within the post-collision field of Pearce (1996) and Be'eri-Shlevin et al. (2009b). The mafic end members of the younger Araba suite (600–560 Ma) are enriched in LILE compared to mafic members of the Aqaba suite, but have a similar REE pattern [$(La/Lu)n$ = 5–15], despite being emplaced in a within-plate tectonic environment. The felsic, granite, end member of the Araba suite has chemical features typical of A-type granite. It is characterized by moderate enrichments in LREE $(La/Sm)_n \sim 2$, flat HREE patterns $(Gd/Lu)_n \sim 1$, and strong negative Eu anomalies ($Eu/Eu^* = \sim 0.07–0.53$) (Jarrar et al., 2003). A-type granitoids in the Aswan area of Egypt dating between 606 and 595 Ma have high Zr, Y, and LREE, and display affinities to shoshonitic magma series (Finger et al., 2008). These tendencies towards enrichments in some trace elements are important for mineralization, discussed in a later section.

The TTG arc-related suite in the Ar Rayn terrane is characterized by weakly fractionated REE patterns with moderately negative Eu anomlies (Doebrich et al., 2007). The high-Al calc-alkaline suite of diorite, granodiorite, and granite displays depleted HREE patterns and no, or positive, Eu anomalies. On average, these rocks are enriched in Rb and Sr, and depleted in Y and Yb relative to the low-Al TTG suite. Both suites plot in the volcanic-arc/syn-collisional granite field of Pearce et al. (1984) consistent with their inferred subduction-related arc setting. The alkali-feldspar granites are generally more evolved than the calc-alkaline rocks, and have strongly fractionated REE patterns with strongly negative Eu anomalies. Like the calc-alkaline rocks, they also plot in the volcanic-arc granite/syn-collisional granite field despite their posttectonic field characteristics, a feature that may have been inherited from the arc-related crust into which they were intruded.

Overall, the variation in REE patterns in the ANS indicates that older CA I-type granitoids formed in equilibrium with residual garnet and that feldspar fractionation played little role in magma genesis. These REE patterns could reflect subduction zone magmagenetic processes or lower crustal melting. In contrast, REE patterns for younger A-type granitoids indicate strong feldspar control and no evidence for residual garnet. These REE patterns strongly implicate low-*P* fractionation processes, perhaps in the upper to middle crust.

The mostly positive values of $\varepsilon_{Nd}(T)$ values of late Cryogenian–Ediacaran granitoids indicate that their magma sources were dominated by juvenile crust and(or) depleted mantle (Moussa et al., 2008). Although tectonic setting may be a fundamental control, as in the case of calc-alkaline melts generated during subduction, the coeval relationship of some calc-alkaline and alkaline suites indicates that calc-alkaline as well as alkaline magmas evolved in anorogenic, post-collisional settings. In these cases, the presence of suites with different chemical affinities may reflect different source rocks rather than different tectonic settings.

The term "A-type" granite originally applied to granite generated in extensional settings along continental rift zones (Loisell and Wones, 1979) but it is now known that A-type granites occur in a variety of settings ranging from within-plate, anorogenic environments to plate boundaries (Bonin, 2007). With regard to their magma origins, one proposal is that they derive from anhydrous high-grade metamorphic rock, for example, granulite that had previously yielded a granitic partial melt (Barker et al., 1975), although it is very hard to understand how such depleted material could generate such enriched melts. Another proposal is that they derive from mafic to intermediate calc-alkaline crust made up of diorite, tonalite, and granodiorite (Anderson, 1983). This model, as applied in the ANS, encompasses the melting of earlier arc rocks followed by anhydrous fractionation giving rise to magmas that retain a calc-alkaline signature (Kessel et al., 1998; Jarrar et al., 2003, 2008), such as the Ar Rayn alkali-feldspar granites, described above. A third model, one which is increasingly applied to Ediacaran ANS and West African granitoids, is that they derive from partial melting of phlogopite-bearing spinel lherzolite perhaps from OIB-type lithospheric–asthenospheric mantle (e.g., Liégois et al., 1998; Jarrar et al., 2008) present in subduction-modified mantle wedges under tectonothermal conditions created by slab break-off or delamination following cessation of subduction (Finger et al., 2008).

Whatever their origin, granites dominate late Cryogenian–Ediacaran magmatism in the ANS. They constitute the most abundant rock type of this period exposed at the surface and, on the basis of seismic refraction data, are inferred to be the main component of the upper 20 km of lithospheric crust in the Arabian Shield (Gettings et al., 1986). The Nubian crustal structure is presumably similar and the structure of both Arabian and Nubian Shields reflects a massive emplacement of granitic magma in the closing stage of evolution of the northern EAO.

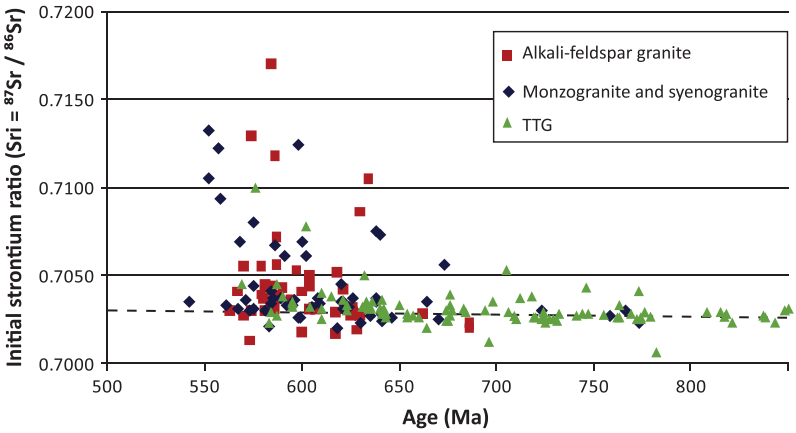

Fig. 14. Initial $^{87}Sr/^{86}Sr$ for plutonic rocks from the Arabian Shield, by general rock type. The TTG series includes diorite, tonalite, trondhjemite, granodiorite, and some gabbro. The data are taken from a table of geochronologic data for the shield compiled by Johnson and Kattan (2007), see for data sources. The dashed line is a Sr-evolution curve indicating a single-stage evolution of depleted mantle from initial $^{87}Sr/^{86}Sr$ of 0.699 at 4.6 Ga to the average modern island-arc value of 0.7037 (adapted from Fleck et al., 1980). The close fit of TTG values to the evolution curve is consistent with the juvenile character of ANS TTG plutonic rocks, which have initial $^{87}Sr/^{86}Sr$ expected for melts formed during the period 850–600 Ma in intraoceanic island arcs. The slightly elevated initial $^{87}Sr/^{86}Sr$ of younger granitic rocks suggests a contribution to the melts from more differentiated sources with higher Rb/Sr, perhaps reflecting partial melting of a thickened crust.

5. Gneiss domes and belts

Gneiss is not widespread in the ANS but is locally present in (1) high-grade parts of arc terranes and Neoarchean–Paleoproterozoic crust in the Abas and Al Mahfid terranes in Yemen (Windley et al., 1996), in the Khida terrane in Saudi Arabia (Stoeser et al., 2001), in the Barka terrane and along the western margin of the Red Sea in Eritrea (Ghebreab et al., 2005); (2) along early to middle Cryogenian sutures zones including the Bi'r Umq–Nakasib suture (Johnson et al., 2003; Hargrove, 2006), the Hulayfah–Ad Dafinah–Ruwah fault zone (Johnson and Kattan, 2001), and the Nabitah fault zone (Stoeser and Stacey, 1988); and (3) as belts and domes of late Cryogenian–Ediacaran gneiss along or close to NW- to WNW-trending fold structures and strike-slip faults in the northern part of the ANS, north-trending shear zones in the southern ANS, and north-trending shortening zones in the Nubian Shield (e.g., Sturchio et al., 1983a,b; El Ramly et al., 1984; Stern et al., 1989; Greiling et al., 1994; Fritz et al., 1996; Fowler and Osman, 2009; Al-Saleh, 2010; Andresen et al., 2010). The late Cryogenian–Ediacaran gneisses are particularly important and are the focus of attention here (Fig. 10).

Late Cryogenian–Ediacaran gneiss in the ANS is chiefly orthogneiss, but in places includes significant paragneiss. The gneiss reflects upper greenschist-amphibolite grade metamorphism under highly ductile to brittle–ductile conditions of deformation. It characteristically consists of mylonitic gneiss containing prominent mineral and stretching lineations and abundant microkinematic shear-sense indicators. Much of the gneiss is probably exhumed ANS middle crust, largely molten because of the magma mush pillow that made up ANS lower crust (Stern and Johnson, 2010), but some, particularly in the Arabian Shield, is likely made up of syntectonic intrusions. In the Arabian Shield, late Cryogenian–Ediacaran gneiss crops out as relatively narrow northwest-trending gneiss belts (Fig. 15). In the Nubian Shield, the gneiss bodies mainly crop out in the cores of structural highs spatially associated with thrust duplexes, strike-slip faults and extensional faults (Fig. 16), and are referred to as gneiss domes or metamorphic core complexes.

5.1. Gneiss belts in the Arabian shield

The longest single gneiss belt in the Arabian Shield is the Hajizah–Tin gneiss, located along the Ruwah fault zone in the eastern shield (Fig. 15B). A series of other belts—the Kirsh, An Nakhil, Wajiyah, and Ajjaj–Hamadat–Qazaz gneisses—form parts of an *en-echelon* Najd fault zone about 1300 km long (referred to as the Qazaz–Ar Rika shear zone) that extends NW across the entire Arabian Shield and continues into the Eastern Desert as the Meatiq, El Sibai, and Hafafit gneiss domes and associated Najd faults (Fig. 10). These gneisses reflect regions along the Najd faults affected by brittle–ductile deformation and greenschist-amphibolite metamorphism; intervening regions were affected by brittle deformation in low grade (greenschist or lower) rocks. This implies that along their strike, the Najd faults pass through several *P*/*T* amphibolite-to-greenschist transitions.

The *Kirsh gneiss belt* (Fig. 15A) consists of an antiform of strongly foliated biotite monzogranite orthogneiss (Al Hawriyah anticlinorium), a belt of steeply dipping kyanite-quartz schist and paragneiss, and subvertical zones of mylonite and ultramylonite (Al-Saleh, 2010). The monzogranite is located in a zone of extension between left-stepping faults along the sinistral Ar Rika shear zone. Left-stepping faults on the southwest side of the shear zone contain a down-faulted section of nonmetamorphosed Jibalah group sedimentary rocks in the Kibdi basin. The Kirsh gneiss has gently NW- and SE-plunging mineral and stretching lineations (Fig. 15A inset). The gneiss is mostly an LS-tectonite, suggesting flattening as well as simple shear, but locally is an L-tectonite, indicating a large component of constriction, or unidirectional stretching. The lineation orientation is replicated in all the Najd-fault gneiss belts in the Arabian Shield and in the gneiss domes in the Eastern Desert and is one of the over-arching structural features of the Najd fault system across the region.

The gneiss belt evolved between about 645 and 590 Ma. Its maximum age is possibly constrained by granite gneiss and pegmatite along the shear zone that have U–Pb SHRIMP crystallization ages of 647 ± 8 Ma (Kennedy et al., 2010) and 637 ± 2 Ma (Kennedy et al., 2005) (Table 3). If the granite is syntectonic, its age would suggest an onset of deformation toward the end of the Nabitah orogeny, during early Murdama deposition. The presence of elongated pebbles in Murdama-group conglomerate (in places, granite pebbles have long axes of 1–2 m) indicates, however, that major ductile deformation in the Kirsh gneiss belt postdated deposition of the Murdama group (~650–625 Ma). Zircon rim overgrowths in the 647 Ma granite gneiss and ~637 Ma pegmatite suggest hydrothermal events between 623 and 589 Ma (Kennedy et al., 2005), consistent with active shearing until about 590 Ma. An

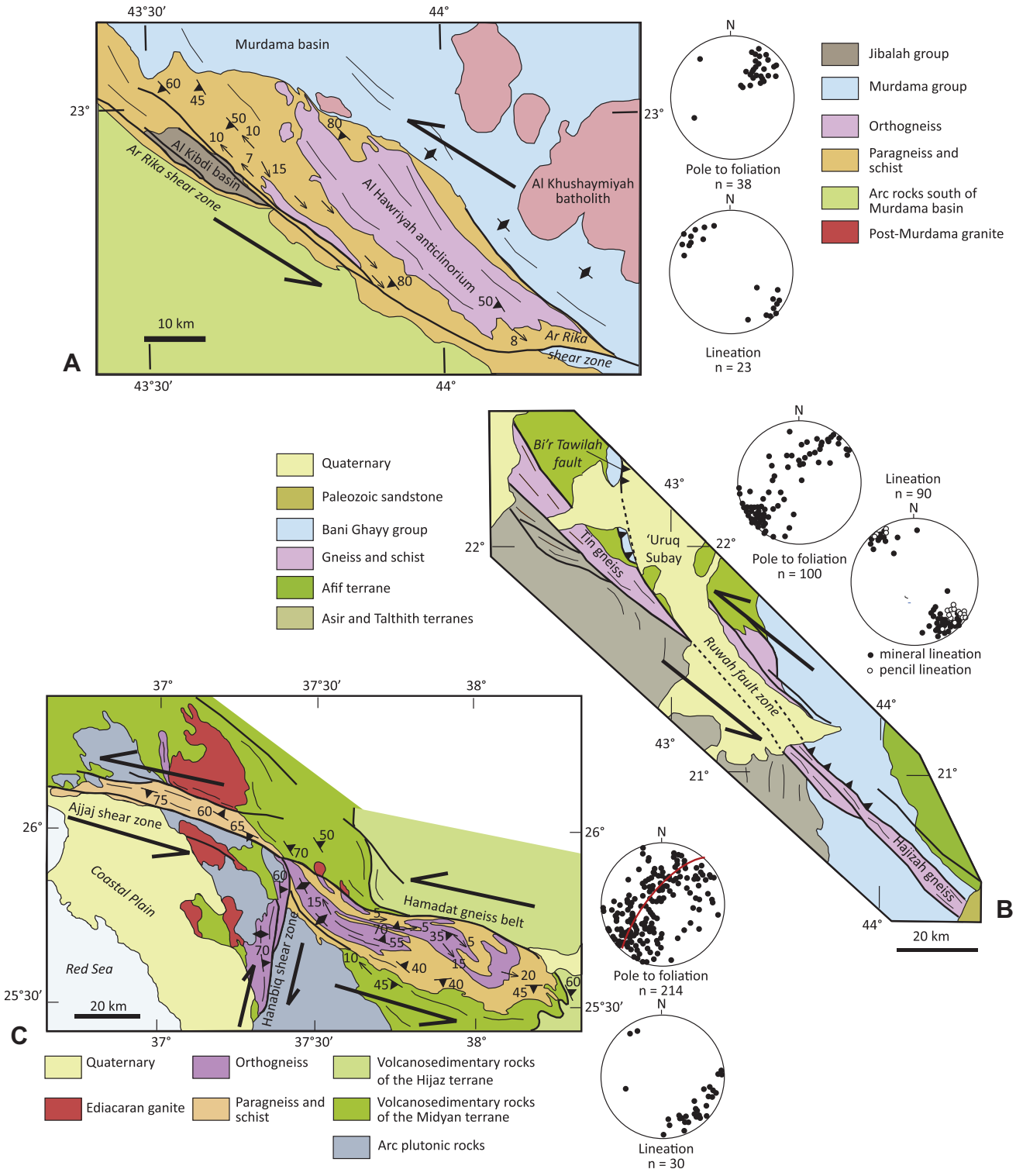

Fig. 15. Simplified geologic maps of selected gneiss belts in the Arabian Shield. A. Kirsh (Al Hawriyah) gneiss belt along the Ar Rika shear zone. B. Hajizah–Tin gneiss belts along the Ruwah fault zone. C. Hamadat gneiss belt and Ajjaj shear zone. Note the consistent NW–SE gentle plunge of lineations throughout the gneiss belts and the broad girdles shown by the plot of poles to foliations for the Hajizah–Tin and Hamadat gneisses suggesting folding of the gneisses. Antiformal structures are reported in the literature for the Al Hawriyah and Hamadat gneisses, but not for the Hajizah–Tin gneiss. See Fig. 10 for locations of these gneiss belts in the ANS.

$^{40}Ar/^{39}Ar$ age of 557 ± 15 Ma obtained from biotite paragneiss is interpreted as the time of cooling below the biotite closure temperature (Al-Saleh, 2010) and the cessation of deformation in the gneiss belt.

The *Hajizah–Tin gneiss belt*, 5–10 km wide and more than 160 km long (Johnson and Kattan, 2001) (Fig. 15B), consists of amphibolite-grade mylonitic orthogneiss, subordinate paragneiss, and minor serpentinite. It crops out along the Ruwah fault zone and may have a complicated history, having undergone initial ductile deformation during the Nabitah orogeny, when the Ruwah fault zone formed part of the Cryogenian suture between the Afif terrane and other terranes to the S, and having undergone

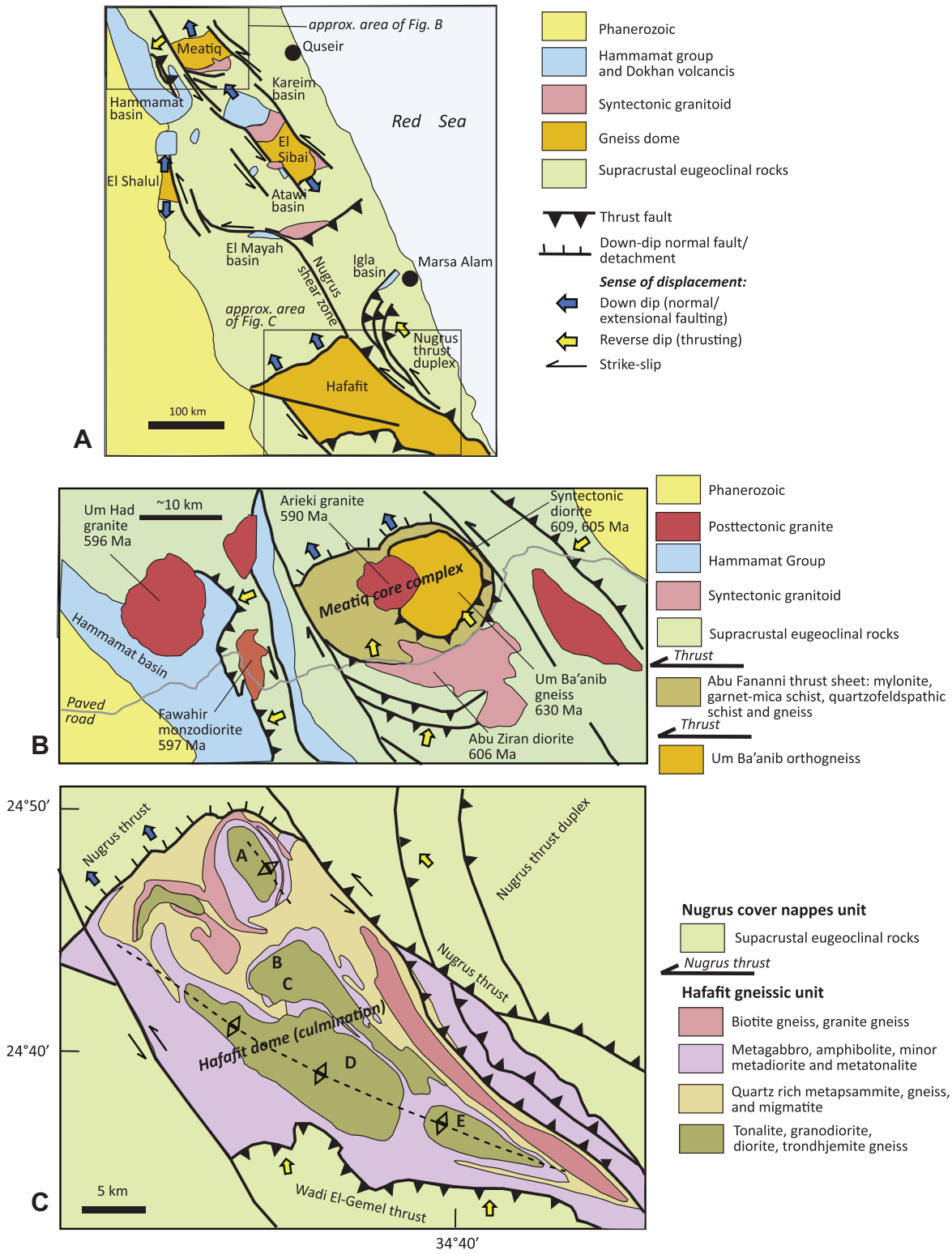

Fig. 16. Gneiss domes in the Eastern Desert, Egypt. (A) Regional structural setting (after Fritz et al. (1996)). (B) Meatiq Dome (after Fritz et al. (1996) and Andresen et al. (2009, 2010)). (C) Hafafit Dome (after Greiling (1997), Abd El-Naby et al. (2008), Shalaby (2010)).

remobilization during late Cryogenian–Ediacaran Najd faulting. Ultramafic rocks are present as lenses, altered by carbonate-rich fluids (listwaenite), along faults at the northern and southern margins of the gneiss belts. SW-verging thrust slices of barely metamorphosed Bani Ghayy group rocks overlie amphibolite on the northeastern side of the gneiss belt, and late- to posttectonic granite and gabbro and mafic and felsic dikes intrude the gneisses. Orthogneiss in the Hajizah gneiss belt is gray, fine-grained to very fine-grained, thinly layered trondhjemite gneiss, tonalite gneiss, quartz diorite, and hornblende diorite gneiss, all with well-developed mylonitic/ultramylonitic fabrics. The rocks are regionally metamorphosed to the almandine-amphibolite facies (Schmidt,

1981) and locally retrogressively metamorphosed along shear zones to epidote–biotite–hornblende assemblages representative of the upper-greenschist facies. The Hajizah gneiss was exhumed prior to overthrusting by the Bani Ghayy group. Both gneiss and overthrust Bani Ghayy group rocks are displaced by brittle sinistral Riedel faults oblique to the main trend of the gneiss belt and intruded by posttectonic dikes, signaling the cessation of brittle–ductile deformation along the Ruwah fault. L-tectonite is locally present, but LS-tectonite is the dominant rock type. Mineral and stretching lineations plunge gently to the NW or SE, comparable to those in the Kirsh gneiss. The maximum age of deformation in the Tin gneiss is constrained by a granodiorite gneiss protolith age of 683 ± 9 Ma (Stacey and Agar, 1985). An Rb–Sr age of 782 ± 26 Ma reported for orthogneiss in the Hajizah gneiss belt (Kröner et al., 1979) may reflect isotopic resetting of an even older protolith formed about 870 Ma. The minimum age of brittle–ductile deformation and metamorphism is constrained by an undeformed "Najd" granite dated 592 ± 4 Ma (Stoeser and Stacey, 1988) that intrudes the gneiss belt. An Rb–Sr potassium feldspar age of 530 ± 20 Ma and a K–Ar plagioclase age of 539 ± 20 Ma obtained from granite gneiss suggests that possible fault-induced isotopic disturbance on the gneiss belt continued as late as the early Cambrian (Kellogg et al., 1986), but such young ages require further confirmation before they are accepted as indicating that tectonic activity continued into Cambrian time. The broad girdle outlined on the plot of poles to foliation in Fig. 15B suggests large-scale folding of the gneiss belt but, unlike the Kirsh gneiss, no megascale antiformal or synformal structure has been observed in the field. Tight mesoscale folds in gneissic foliation are locally present, plunging gently SE and NW parallel to the observed lineations, but the belt as a whole has the appearance of a steeply dipping homocline.

High-grade rocks along the *Qazaz* and *Ajjaj shear zone* and *Hamadat gneiss belt* (Fig. 15C) include hornblende gneiss, tonalite gneiss, granodiorite gneiss, and granite gneiss. Strongly deformed volcanic and sedimentary rocks include quartzofeldspathic schist, amphibolite and amphibole schist, migmatite of alternating quartzofeldspathic and amphibole schist, garnet- and kyanite-bearing schist, and schistose volcanic rocks. Abundant S–C and S–C′ fabrics and rotated porphyroclasts consistently indicate a sinistral sense of shear. The maximum age of ductile deformation and high-grade metamorphism is not well constrained, but the presence of strongly elongated pebbles demonstrates that much searing postdated deposition of the Thalbah group (660–620 Ma). Ductile deformation continued until at least 575 Ma, the protolith age of granite gneiss on the northern margin of the Ajjaj shear zone, but ceased very shortly after that, prior to the intrusion of undeformed 573 Ma lamprophyre dikes (Kennedy et al., 2011). The Ajjaj shear zone and Hamadat gneisses are strongly foliated and lineated with lineations plunging gently SE and NW. L–S fabrics predominate but L-tectonites are locally present. Poles to foliation in the Hamadat gneiss (Fig. 15C) define a broad girdle, compatible with the map-scale anticlinorium that has been mapped in the gneiss, and broad antiformal structures are found in part of the Qazaz gneiss.

The northwest-trending Ajjaj shear zone is notable for its intersection with the north-trending *Hanabiq* dextral shear zone and *Baladiyah* gneiss (Fig. 15C), although the temporal and structural relationships between the gneisses and shear zones are yet to be fully established. Duncan et al. (1990) concluded that the Hanabiq shear zone is a continuation across the Red Sea of the Hamisana shear zone of the Nubian Shield (location shown in Fig. 10) and that the Ajjaj crosscuts the Hanabiq. Alternatively, the Hanabiq may form a "zipper" shear with the Ajjaj shear zone (Passchier, 2010). The Baladiyah gneiss has a protolith age of 676 Ma (conventional U–Pb zircon age; Hedge, 1984), indicating that the magmatic rock forming the gneiss was in place prior to movement on the Ajjaj shear zone. Overgrowth rims on zircons in the Baladiyah gneiss at 610 Ma may date metamorphism accompanying movement on the Ajjaj shear zone (Kennedy et al., 2010).

5.2. Late Cryogenian–Ediacaran gneisses in the Eastern Desert and Sinai

Gneisses on the Qazaz–Ajjaj shear zone continue into the Central and South Eastern Desert of Egypt as gneiss domes at Meatiq, El Sibai, and Hafafit (Fig. 16) (Sturchio et al., 1983a; Greiling et al., 1994; Fritz et al., 1996; Fowler and Osman, 2001; Bregar et al., 2002; Andresen et al., 2009). The gneiss domes are polydeformed, polymetamorphosed (Neumayr et al., 1998), and lithologically complicated. As a consequence, their origin, age, structure, and tectonic implications are debated. Nonetheless, all workers recognize that they are important to our understanding of ANS geology because they are windows into the structural infracrust and deeper part of the region and are at the heart of the debate about the presence or not of "older basement" in the region. In the early and "classical" Egyptian literature, the orthogneiss in the cores of the gneiss domes is considered to be an extension of the middle-Proterozoic crust exposed in the Western Desert of Egypt (e.g., El-Gaby et al., 1988, 1990) or derived by partial melting of such crust (Khudeir et al., 2008). However, there is a growing body of robust geochronologic and isotopic data that indicates the gneisses are variably deformed calc-alkaline Neoproterozoic intrusions and juvenile arc-related Neoproterozoic crust of the ANS (e.g., El Ramly et al., 1984; Greiling et al., 1984, 1988; Kröner et al., 1987; Andresen et al., 2009; Liégeois and Stern, 2010).

Many structural features of the Egyptian gneiss domes are similar to those in the gneiss belts exposed in the Arabian Shield. They have subhorizontal NW–SE-trending stretching lineations that are parallel in some cases to the overall dome axes. The dip of foliation is steep along the southwestern and northeastern dome margins and flat within the dome cores defining apparent antiforms (Fowler and Osman, 2001; Andresen et al., 2010). All of the domes are broadly aligned along a northwest-trending system of ductile to brittle shear/fault zones, referred to as the "Najd Corridor" (Fritz et al., 1996), which most workers correlate with the Najd fault system in the Arabian Shield. Both the Arabian Shield gneiss belts and the Eastern Desert gneiss domes evidence NW-directed extension. In the Arabian Shield, the evidence consists of pervasive stretching lineations and elongated sedimentary clasts (pebbles). In the Eastern Desert the evidence consists of normal faults and shear zones that developed predominantly along the northwestern and/or southeastern dome margins, and around depositional basins that evolved close to the domes, particularly adjacent to the bordering fault zones (Fritz et al., 2002). It should be noted, however, that the structural relationships of the gneiss domes are not always clear and are the subject of debate because different segments of the shear-extension system hosting the domes were affected by different amounts of displacement and strain partitioning (Fritz et al., 2002). As a consequence, some authors interpret the high-strain zones around the domes to be low-angle detachment faults; others consider the structural contacts to be the remnants of NW-directed thrusts (Andresen et al., 2010). Some authors envisage the domes to be controlled by extension in the "Najd-fault corridor" with normal faults representing extensional bridges or releasing steps between strike-slip Najd faults (Fritz et al., 2002). Still others treat the northwest-trending faults around the gneiss domes as due to later deformation superimposed on earlier high-strain zones.

Despite a lack of agreement about details, however, a general structural model for the evolution of the Egyptian gneiss domes has emerged. The model envisages an early phase of hanging wall displacement toward the northwest, possibly at the time of terrane accretion in the Eastern Desert, which emplaced ophiolite-bearing

Table 3
Geochronologic constraints on Najd faulting: a list of intrusive and(or) sedimentary and volcanic rocks that predate, postdate, are cut by, or are deformed by Najd faults and thereby help to constrain movements on the faults.

Age	Unit dated	Method	Fault zone affected	Comment	Source
591 ± 6	Undeformed "Najd granite"	U–Pb zircon Concordia method	Ruwah fault zone	A massive granite that intrudes the Ruwah fault; constrains cessation of movement on the fault	J.S. Stacey, written communication, 1983; cited by Kellogg et al. (1986)
Qazaz–Ajjaj shear zone					
705 ± 4	Zaam group paragneiss	U–Pb, SHRIMP	Qazaz–Ajjaj	Predates deformation on Ajjaj shear zone	Kennedy et al. (2010a, 2011)
670 ± 10	Hamadat diorite gneiss	U–Pb, SHRIMP	Qazaz–Ajjaj	Pre-dates Najd deformation	Kennedy et al. (2004)
630 ± 19	Raydan pluton	Rb–Sr	Qazaz–Ajjaj	Granite cataclastically deformed by Najd faulting: age probably reflects open isotopic system and perhaps the onset of active faulting	Kemp et al. (1980)
626 ± 4	Abu Suar complex; granite	U–Pb, SHRIMP	Qazaz–Ajjaj	Predates deformation on Qazaz shear zone	Kennedy et al. (2011)
609 ± 4	Ash Sha'b complex	U–Pb, SHRIMP	Qazaz–Ajjaj	Suspect syntectonic granite: massive immediately north of shear zone; altered to mylonitic gneiss within the shear zone: implies ductile deformation about or soon after 609 Ma	Kennedy et al. (2011)
599 ± 5 (core) 570 ± 5 (rim)	Jibalah group, Dhaiqa formation	U–Pb, SHRIMP	Qazaz–Ajjaj	Possible age of igneous zircon, implying deposition </= 599 Ma. Constrains brittle Najd deformation	Kennedy et al. (2011)
575 ± 10	Foliated granite on margin of Ajjaj shear zone		Qazaz–Ajjaj	Suspect syntectonic granite, synchronous with ductile deformation on Ajjaj shear zone	Kennedy et al. (2011)
573 ± 6	Undeformed lamprophyre dikes cross cutting Ajjaj shear zone gneiss		Qazaz–Ajjaj	Constrains cessation of ductile deformation on Ajjaj shear zone	Kennedy et al. (2011)
560 ± 4	Jibalah group, Dhaiqa formation		Qazaz–Ajjaj	Age of igneous zircon; constrains maximum deposition age and timing of brittle Najd deformation	Vickers-Rich et al. (2010)
Halaban-Zarghat					
624.9 ± 4.2	Murdama rhyolite: basement of Jifn basin	U–Pb	Halaban-Zarghat	Maximum age of formation of basin and initiation of dextral movement on Halaban-Zarghat fault	Kusky and Matsah (2003)
621 ± 8	An Nimriyah pluton: hornblende–biotite quartz monzodiorite	U–Pb	Halaban-Zarghat	Crystallization age: similar plutons in the area intrude Najd fault; implies onset of faulting predates 621 Ma	Cole and Hedge (1986)
621 ± 7	Mushrifah pluton: biotite–hornblende quartz diorite	U–Pb	Halaban-Zarghat	Pluton is cut by the Halaban-Zarghat fault; similar rocks exposed 10 km to the west on south side of fault: indicates right-offset after emplacement, and implies a <621 Ma period of dextral shearing	Cole and Hedge (1986)
620 ± 7	Al Asfah pluton: hornblende–biotite quartz monzodiorite (Idah suite)	U–Pb	Halaban-Zarghat	Truncates NW-trending splay faults that connect with Halaban-Zarghat fault: indicates offset on the splays had ended by about 620 Ma. Inferred that major transcurrent movement predates Idah suite, i.e. >620 Ma	Cole and Hedge (1986)
588 ± 12	Jabal Tukhfah granite	Rb–Sr	Halaban-Zarghat	May postdate Najd faulting; constrains cessation of movement	Fleck and Hadley (1982)
574 ± 28	Ar Rahadah pluton: alkalki-feldpsar granite	Rb–Sr	Halaban-Zarghat	Intrudes Murdama group and cut by Najd fault	Calvez et al. (1984)
576.6 ± 5.3	Undeformed felsite dike	U–Pb	Halaban-Zarghat	Intrudes Jibalah group in Jifn basin; gives a minimum age for movement on Halaban-Zarghat fault	Kusky and Matsah (2003)
573 ± 8	Habariyah monzogranite gneiss	U–Pb, SHRIMP	Halaban-Zarghat	Suspect syntectonic granite: 573 Ma is inferred main crystallization event: granite underwent hydrothermal alteration between 531–512 Ma. Constrains ductile deformation as 573 Ma or younger	Kennedy et al. (2005)
566 ± 8	Jibalah group (Antaq basin)	LA-ICP-MS	Halaban-Zarghat	Maximum deposition age; faulting active	Nettle (2009)
568 ± 11	Jibalah group (Antaq basin)	LA-ICP-MS	Halaban-Zarghat	Maximum deposition age; faulting active	Nettle (2009)
584 ± 10	Jibalah group (Antaq basin)	LA-ICP-MS	Halaban-Zarghat	Maximum deposition age; faulting active	Nettle (2009)
Ar Rika					
601 ± 4	Dahul granite	U–Pb	Between Ar Rika and Ruwah faults	Cut by brittle fault; implies brittle deformation as late as 601 Ma	Aleinikoff and Stoeser (1988)
579 ± 19	Kursh granite	Rb–Sr	Between Ar Rika and Ruwah faults	Cut by brittle fault; implies brittle deformation as late as 579 Ma	Calvez et al. (1983)
637 ± 2	Pegmatite in Kirsh granite gneiss	U–Pb, SHRIMP	Ar Rika	Possibly main crystallization event at ~637 Ma: subsequent recrystallization (metamorphic?) events between 623 and 589 Ma; constrains ductile deformation	Kennedy et al. (2005)
~600	Kirsh granite gneiss	U–Pb, SHRIMP	Ar Rika	A possible metamorphic age; consistent with ductile deformation at ~600 Ma	Kennedy et al. (2005)
~620–580	Kirsh granite gneiss	U–Pb, SHRIMP	Ar Rika	Possible crystallization age range	Kennedy et al. (2005)

(*continued on next page*)

Table 3 (*continued*)

Age	Unit dated	Method	Fault zone affected	Comment	Source
731 ± 8	An Nakhil gneiss: granite	U–Pb, SHRIMP	An Nakhil shear zone, part of Ar Rika-Qazaz system	Pre-dates Najd deformation	Kennedy et al. (2004)
567 ± 86	Abu Aris granite			Cut by Najd faults; implies brittle deformation as late as 567 Ma	Fleck and Hadley (1982)
632 ± 15	Haml suite: Awjah complex	U–Pb		Pluton cut by Najd fault; constrains maximum age of faulting	Stacey and Agar (1985)
632 ± 3	Hufayrah complex: alkali-feldspar granite	U–Pb		Pluton cut by Najd fault; constrains maximum age of faulting	Stacey and Agar (1985)
577 ± 21	Sanam pluton	Rb–Sr		Crystallization age is 607 ± 18 Ma: a younger age of 577 Ma reflects open isotopic system, consistent with active faulting	Calvez et al. (1983)
647 ± 8	Granite gneiss	U–Pb, SHRIMP	Ar Rika	Crystallization age about 647 Ma; subsequent thermal event about 600 Ma	Kennedy et al. (2011)
611 ± 3	Uwaiyjah complex	U–Pb	Ar Rika	Granodiorite immediately north of fault zone; If syntectonic, implies active faulting ~611 Ma; if posttectonic implies cessation of shearing and ductile prior to 611 Ma	Agar et al. (1992)

volcanosedimentary suites (supracrust) onto deeper parts of the crust (infracrust). The supracrustal rocks are part of the larger northwestward-verging thrust duplex of juvenile Neoproterozoic island-arc, sedimentary, and volcaniclastic rocks together with ophiolite fragments that make up most of the Eastern Desert. The infracrust contains calc-alkaline Neoproterozoic intrusions that underwent complex folding and thrusting and were transformed into gneiss that is exposed in dome cores. Other gneisses in the domes represent syntectonic intrusions emplaced during subsequent periods of northward displacement of the hanging wall. The juxtaposition of low-grade island-arc sequences of the hanging wall along a high strain zone against the intermediate and high-grade gneiss of the footwall indicates crustal scale thinning, best explained by extensional faulting, rather than thrusting (Fowler and Osman, 2009; Andresen et al., 2010). A distinctive recent interpretation is that the gneisses up-domed vertically through nappes of overthrust low-grade volcanosedimentary rocks of the Pan-African cover, having been previously emplaced during accretion of the nappes (Shalaby, 2010).

Ongoing convergence and Najd transpression buckled the infracrust and the high-strain zone between the infracrust and supracrust resulting in the emergence of domes with a general northwest-trending orientation. Along dome margins, oblique convergence partitioned into strike-slip and normal faults, most probably triggered by pronounced rheologic contrast between updomed gneissic infracrust and the rheologically weaker volcanosedimentary supracrust. Strike-slip faults developed preferentially on southwestern and northeastern dome margins (Fig. 16A and B), although this interpretation is subject to debate (Fowler and Osman, 2001; Andresen et al., 2010). In places, the domes are associated with oblique strike-slip thrust faults that evidence a significant vertical component of flow (Fig. 16C), and normal faults developed on northwestern and southeastern dome margins (Fig. 16A and B). This allowed for general NW–SE extension, causing dome exhumation and the development of intermontane basins such as the Kareim basin (Fig. 16A). Shear along strike-slip faults flanking the gneiss domes was generally sinistral. However, depending on specific local conditions and strain partitioning, different types of displacement may be observed such as shear reversal during dome exhumation, dextral shear, and normal (extensional) faulting (Andresen et al., 2010).

The initiation of extensional tectonics in the Eastern Desert may be determined by: (1) the ages of pre-, syn- and posttectonic plutons that intrude the gneiss domes; (2) the structural relations between the gneiss domes and sedimentary basins; and (3) direct dating of deformation, metamorphism, and general cooling of the domes. Although a diachronous evolution is suggested (Fritz et al., 2002), geochronologic work by Andresen et al. (2009) suggests, as a general model, that exhumation commenced around 620–606 Ma (oldest $^{40}Ar/^{39}Ar$ cooling ages and emplacement of extension related Abu Ziran granitoid), continued at intermediate crustal level for about 49 m.y., and ceased prior to emplacement of discordant posttectonic granitoids at about 580 Ma (see below for arguments from individual areas). It should be noted, furthermore, that most of the sedimentary rocks deposited within post-amalgamation Hammamat Group basins close to the gneiss domes are deformed, clearly indicating that shearing outlasted this sedimentation (Fowler and Osman, 2001; Abdeen and Greiling, 2005; Abdeen et al., 2008).

The geodynamic setting of the gneiss domes is a matter of discussion. Analogies have been drawn, on the one hand, with classic metamorphic core complexes, invoking gravitational collapse and extrusion tectonics (“extensional settings”) and, on the other hand, with an interplay between thick-skinned and thin-skinned thrusting (“compressional settings”). Aside from the fact that extensional and compressional settings may coexist during orogeny (in this case, Najd shearing), understanding the driving mechanism requires knowledge about the general state of the late Neoproterozoic lithosphere in the region of what is now the EAO. It is particularly important to understand: (1) the relative contribution of body (gravitational) forces versus boundary (plate) forces; (2) the configuration of plate boundaries, particularly the boundary of the entire EAO against paleoTethys and whether this was a zone of subduction or extension; and (3) the thermal state of the lithosphere. These issues will be considered in more detail in a forthcoming review of the EAO by H. Fritz and colleagues.

The *Meatiq Dome* (or core complex) (Sturchio et al., 1983a,b; Loizenbauer et al., 2001; Andresen et al., 2009, 2010) (Fig. 16B) consists of two units of quartzofeldspathic gneiss, schist, and mylonite—the Um Ba’anib orthogneiss and the Abu Fananni thrust sheet—structurally overlain by supracrustal rocks (island-arc volcanics, sedimentary rocks, and ophiolitic rocks) belonging to the typical juvenile crust of the Eastern Desert. Andresen et al. (2009) refer to the overlying rocks as a “eugeoclinal thrust sheet”. The dome is an oval outcrop about 25 km WSW–ENE and 15 km NNW–SSE comprising an asymmetric doubly plunging antiform trending NW–SE to NNW–SSE. The Um Ba’anib orthogneiss (630 Ma; Andresen et al., 2009), in the core and forming the lowest structural level of the dome, consists of recrystallized granitoid of possible granodiorite origin (Andresen et al., 2009). The overlying Abu Fananni thrust sheet consists of variably deformed and mylonitized intrusive and subordinate sedimentary rocks comprising garnet-mica schist and quartzofeldspathic gneiss and schist (Habib et al., 1985). The contact between the Um Ba’anib gneiss and Abu

Fananni thrust sheet is a zone of mylonite 100–200 m thick. The two may originally have had a quasi-depositional relationship, but kinematic indicators demonstrate that the Abu Fananni thrust sheet has been translated to the northwest over the Um Ba'anib orthogneiss (Loizenbauer et al., 2001; Andresen et al., 2009, 2010). The Um Ba'anib and Abu Fananni rocks contain conspicuous NW–SE to NNW–SSE-trending stretching lineations formed under conditions of amphibolite facies metamorphism and sparse kinematic indicators indicating top-to-the-NW displacement (Sturchio et al., 1983a,b; Andresen et al., 2009). The overlying ophiolitic and volcanosedimentary supracrustal rocks are separated from the underlying gneissic rocks by a high-strain zone referred to as the Eastern Desert Shear Zone (EDSZ) (Andresen et al., 2010). It is a top-to-the-NW shear zone (Fritz et al., 1996; Fowler and Osman, 2001; Fowler and El Kalioubi, 2004; Andresen et al., 2009). The EDSZ is intruded by the syntectonic Abu Ziran diorite (606 ± 1 Ma) (Andresen et al., 2009). Hammamat Group sedimentary rocks 20 km west of the Meatiq Dome are partly unconformable on and partly overthrust by the supracrustal rocks. Fritz et al. (1996) argue that the thrust-emplacement of supracrustal rocks over the Hammamat group reflects W- to SW-tectonic transport, which was contemporary with the NW-transport of the eugeoclinal thrust sheet at the Meatiq Dome itself, and is evidence of strong regional strain partitioning in this part of the Central Eastern Desert. It may, alternatively, reflect progressive deformation and a switch from NW-directed extension to transpression associated with bulk E–W shortening. The Hammamat rocks themselves were folded and overthrusted prior to intrusion of the posttectonic Um Had granite (596 ± 2 Ma) (Andresen et al., 2009) (Fig. 16B).

The Meatiq Dome is commonly viewed as being overprinted by northwest-trending strike-slip faults on the east and west and by gently dipping normal faults on the south and north (e.g., Fritz et al., 1996). Those on the east and west are steep, NW- to NNW-trending shears interpreted by most workers as a pair of sinistral Najd faults (e.g., Loizenbauer et al., 2001) that continue from the Arabian Shield as an extension of the Qazaz shear zone, and were active during exhumation of the dome. Andresen et al. (2010) report, however, that the shear zone on the northeastern flank of the dome is left lateral whereas that on the southwestern flank is right lateral, which is not compatible with the shear zones being part of a "Najd corridor". Instead, Andresen et al. (2010) argue that the shear zones are the effect of folding the EDSZ about a NW-trending axis. Either model, nonetheless, implies NE–SW shortening and NW–SE extension. In this context, the warning by Fowler and Osman (2001) is apposite, that "caution must be exercised in the recognition of transcurrent shears in the Eastern Desert since folded low-angle thrust-related mylonitic zones may be steepened by folding, producing steep shear zones with low-pitching slip lineations" (pg. 17). Lateral shear together with NW–SE extension is suggested from the intermontane Kareim basin, south of the Meatiq Dome (Fig. 16A). The basin is bound by northwest-trending steep shear zones and NW-dipping normal faults (Fritz and Messner, 1999), reflecting general NW–SE extension. NW–SE extension is viewed as causing the exhumation of high-grade infracrustal rocks into the core of the dome, concurrent with sinistral strike-slip shearing on the eastern and western margins, the emplacement of syntectonic granitoids, and NE–SW contraction (Fritz et al., 1996, 2002; Fritz and Messner, 1999). The southern Kareim basin is intruded by a posttectonic granitoid (Al Dabbah granodiorite: Fowler et al., 2007) causing contact metamorphism of basal strata of the sedimentary succession in the Kareim basin. This could narrow down the time of sedimentation but unfortunately this magmatic body is not dated.

Um Ba'anib gneiss protolith ages range from 779 ± 4 Ma ($^{207}Pb/^{206}Pb$ dating of an evaporated single zircon; Loizenbauer et al., 2001) to 626 ± 2 Ma (Rb–Sr whole-rock isochron; Sturchio et al., 1983b), but a recent ID-TIMS age of 630.8 ± 2.0 Ma obtained from dating of two fractions of zircon is possibly the most reliable crystallization age (Andresen et al., 2009). The 630 Ma age of emplacement of the Um Ba'anib orthogneiss protolith provides a maximum age for the ductile fabric recorded in the Um Ba'anib gneiss. The timing of ductile deformation in the Abu Fananni thrust sheet, which may reflect the time of northwestward displacement of the Abu Fananni thrust sheet (Andresen et al., 2009) or onset of younger extension, is constrained by syntectonic diorite dated at 609 ± 1.0 Ma and 605.8 ± 0.9 Ma (Andresen et al., 2009). The minimum age of the Um Ba'anib gneiss-forming event, as well as the minimum age for juxtaposing the Um Ba'anib and Abu Fananni gneisses, is constrained by the posttectonic Arieki granite (590.5 ± 3.1 Ma: Andresen et al., 2009) that intrudes the Um Ba'anib orthogneiss and Abu Fananni thrust sheet. The age of the main shearing in the region that emplaced the supracrustal rocks over the infracrustal gneisses in the Meatiq Dome is constrained by the interpretation adopted for the Abu Ziran diorite (606 ± 1 Ma). Andresen et al. (2009) interpret the diorite as a syntectonic intrusion into the mylonitic gneisses along the contact between the Abu Fannani thrust sheet and the supracrustal rocks and conclude that the supracrustal rocks were translated over the gneissic rocks prior to about 606 Ma. The Abu Ziran pluton, alternatively, has been interpreted as a magmatic body emplaced during extension and exhumation of the Meatiq Dome and coeval with southward displacement of its low-grade structural cover (Fritz and Puhl, 1997). The $^{40}Ar/^{39}Ar$ ages of white mica from the extensional shear zone at the southern margin of the Meatiq Dome indicate that NW–SE extension was initiated by 585 Ma (Fritz et al., 1996). The minimum age of sedimentation and deformation in the Hammamat basin west of and external to the Meatiq Dome is constrained by the posttectonic Um Had granite (596.3 ± 1.7 Ma) (Andresen et al., 2009), which intrudes the Hammamat and supracrustal rocks that were thrust westward over the Hammamat (Fig. 16B). Because the Um Had granite is not in contact with the Meatiq Dome, however, the age of the granite does not necessarily constrain the end of deformation in the internal part of the dome or in the "Najd corridor" flanking the dome. Taking the available geochronology into account, Andresen et al. (2009) concluded that the Meatiq Dome represents a young structural feature (<631 Ma) and that shearing and concurrent sedimentation and magmatism within and around the dome took place in a relatively short interval between 610 and 595 Ma. The timing of final exhumation of the Meatiq Dome is constrained by hornblende and white mica $^{40}Ar/^{39}Ar$ ages between 587 Ma and 579 Ma obtained from the Um Ba'anib orthogneiss (Fritz et al., 2002), close to the 590 Ma intrusion age of the posttectonic Arieki granite. The $^{40}Ar/^{39}Ar$ ages are interpreted as the time of cooling below the blocking temperatures for hornblende and white mica, respectively, and the timing of rapid exhumation of the dome.

Like the Meatiq Dome, the *Hafafit Dome* (or culmination) also comprises a structural high made up of high-grade orthogneiss and paragneiss flanked and structurally overlain by low-grade supracrustal rocks. The high-grade rocks, referred to as the Hafafit gneissic unit (Abd El-Naby et al., 2008; Shalaby, 2010), include (1) up to five separate small domes of tonalitic and trondhjemitic gneiss (lettered A–F in Fig. 16C); (2) a heterogeneous unit of metagabbro, massive and foliated amphibolite, minor metadiorite, and metatonalite; (3) quartz-rich metapsammite, metapsammitic gneiss, and migmatite; and (4) biotite-rich gneiss and granite gneiss. Structurally, the tonalitic and trondhjemitic domes and other rocks are a set of interference folds locally involving migmatites (Greiling et al., 1994; Fowler and El Kalioubi, 2002). The overlying low-grade supracrustal rocks, referred to as the Nugrus unit and equivalent to the supracrustal rocks flanking the Meatiq Dome,

consist of low-grade mica schist, metavolcanics, serpentinite, and metagabbro. They are separated from the high-grade rocks of the dome on the east by a steeply dipping shear zone (the Nugrus thrust) with a significant component of sinistral strike slip evidenced by a thick mylonitic zone (Greiling et al., 1988; El Ramly et al., 1984). Fowler and Osman (2009) model this mylonite zone as a folded low-angle extension-related normal shear. On the south and southwest, the Hafafit gneisses are bounded by the low-angle Wadi El-Gemel thrust, on the west by a NW-tending sinistral strike slip fault, and on the north by a low-angle normal fault. The granitic gneisses in the core of the Hafafit dome have been interpreted as pre-Neoproterozoic basement (El-Gaby et al., 1984, 1988) but U–Pb dating of zircons yield a crystallization age of 682 Ma or less (Stern and Hedge, 1985; Lundmark et al., 2011) demonstrating that the high-grade rocks are ANS juvenile crust. Whole-rock samples of biotite gneiss, hornblende gneiss, and amphibolite and garnet and plagioclase mineral separates yield Sm–Nd ages of 593 ± 4 and 585 ± 8 Ma, which are interpreted as the timing of cooling and exhumation following peak metamorphism (Abd El-Naby et al., 2008) consistent with $^{40}Ar/^{39}Ar$ ages of 586.1 ± 0.3 Ma and 584.2 ± 0.2 Ma obtained by Fritz et al. (2002) for hornblende separates from the dome. A slightly younger Sm–Nd age of 573 ± 6 Ma may reflect a later stage of cooling (Abd El-Naby et al., 2008). Garnet–biotite, garnet–amphibole, and amphibole–plagioclase geothermometry yields temperatures of 600–750 °C for metamorphism in gneiss and amphibolite within the Hafafit dome, and garnet-hornblende-plagioclase-quartz geobarometry suggests pressures of 6–8 kbar. Nd and Sr isotopic data also indicate that Hafafit gneisses represent juvenile Neoproterozoic crust (Liégeois and Stern, 2010).

In Sinai, late Cryogenian layered gneiss and associated syntectonic granodiorite referred to as the *Feiran–Solaf metamorphic belt* (Fowler and Hassen, 2008) crop out in the Wadi Feiran area as a series of northwest-trending anticlines overturned to the west and separated by northwest-trending thrust faults (El-Shafei and Kusky, 2003). The rocks are referred to in the literature as paragneiss (Akkad et al., 1967a,b) but low $^{87}Sr/^{86}Sr$ (0.7034–0.7039) suggests that the protoliths were very immature, volcanogenic wacke or lithic wacke interbedded with felsic tuffs (Stern and Manton, 1987). The gneiss has been dated using Rb–Sr whole-rock techniques at 643 ± 41 Ma (Bielski, 1982) and 614 ± 27 Ma (Stern and Manton, 1987), who also report a thin-layer Rb–Sr age of 610 ± 44 Ma. Conventional U–Pb dating of a single fraction of zircon yields an age of 632 ± 3 Ma (Stern and Manton, 1987). The U–Pb age may approximate the age of the protolith or the age of the crust sampled by protolith sediments, and the Rb–Sr ages may approximate the age of metamorphism and deformation that formed the gneiss (Stern and Manton, 1987). Clearly the Feiran gneiss formed in early Ediacaran times, as further indicated by a 591 ± 9 Ma (Rb–Sr whole-rock) posttectonic dike, which gives a minimum age for Feiran gneiss formation (Stern and Manton, 1987). The Feiran gneiss defines one of the most striking crustal boundaries in the ANS, separating early Cryogenian and latest Mesoproterozoic crust to the northeast from late Cryogenian and younger crust to the southwest, all intruded by Ediacaran igneous rocks. Evidence of much older crust was first recognized as relatively undeformed granodiorite with a discordant 3-fraction conventional U–Pb age of 782 ± 7 Ma that lies just to the east of the northwest-trending gneiss belt (Stern and Manton, 1987). Similar igneous rocks are recognized in this region, including the 844 ± 4 Ma Moneiga quartz-diorite (Bea et al., 2009). The ~610 Ma age of Feiran gneiss metamorphism, its NW trend, and subhorizontal lineations (Fowler and Hassen, 2008) and the fact that it separates an unusually old tract of early Cryogenian igneous rocks from younger Cryogenian basement to the west suggest that the Feiran gneiss belt is related to Najd deformation (Abu-Alam and Stüwe, 2009).

The Feiran–Solaf gneisses reflect relatively low *P*–high *T* amphibolite facies conditions. Eliwa et al. (2004) estimated $T \sim 638$–677 °C and *P* of 4–5 kbar for the Solaf zone biotite-hornblende gneisses, whereas Abu Alam et al. (2010) determined conditions of 7–8 kbar at $T \sim 600$–720 °C for the amphibolite-facies calc-silicate rocks. Overall, the Feiran gneisses originated during a single metamorphic cycle, with peak metamorphism at 700–750 °C and 7–8 kbar and subsequent isothermal decompression to ~4–5 kbar, followed by cooling to 450 °C (Abu-Alam and Stüwe, 2009). Cooling and structural shortening were synchronous and associated with Najd-related exhumation of the complex during an episode of oblique transpression. The *P–T* estimates for Feiran peak metamorphism indicate Ediacaran T gradients of several tens of °C/km, consistent with a partially molten mafic lower crust, at $T \sim 1100$–1300 °C. Gneissosity in the area developed during an early (D_1) phase of deformation (El-Shafei and Kusky, 2003) interpreted as an extensional tectonic event and underwent as many as three subsequent folding events (Fowler and Hassen, 2008).

Ninety km SE of the Feiran–Solaf area, the Sinai region contains a metamorphic core complex that is likewise interpreted as the result of extension during Ediacaran orogenic collapse (Blasband et al., 1997). Unlike the domes described above, however, the *Wadi Kid core complex*, as it is referred to, is identified by gently dipping mylonitic foliation and gently plunging mineral and elongation lineations in schistose metasedimentary rocks, not gneiss. The foliations defined a subhorizontal mylonitic zone as much as 1.5 km thick. Shear sense indicators give a consistent regional transport direction to the northwest, with local reversals to the southeast. Metamorphism in the mylonitic zone is of the LP/HT type (Shimron, 1987), and the foliated formations were formed at a depth of at least 10 km (Reymer et al., 1984). Two main periods of deformation are recognized in the rocks. The earlier, >620 Ma, D_1 event is related to compression associated with island-arc subduction. The D_2 event (620–580 Ma) was associated with extension and was responsible for development of the mylonitic foliation superimposed on D_1 structures. Non-coaxial deformation during D_2 indicates top-to-the-NW transport of the rocks overlying the mylonitic zone; reversal of movement to the SE was caused by subsequent upwarping due to the intrusion of late Ediacaran granitoids (560–530 Ma) (Blasband et al., 1997). The transition from D_1 compression to D_2 extension was due to orogenic collapse.

6. Middle Cryogenian–Ediacaran arc- and terrane-forming events

The distinctive geology of the Ad Dawadimi and Ar Rayn terranes located along the eastern edge of the Arabian Shield (Fig. 8) has been referred to earlier in this review (Section 4.3). The terranes are important because: (1) they are the youngest terranes in the ANS; (2) they provide evidence for subduction in the Ediacaran, well after other terranes had already amalgamated; (3) their mutual juxtaposition represents the youngest suturing event in the ANS; and (4) their juxtaposition with terranes to the west reflects the final closure of the Mozambique Ocean and the convergence of Neoproterozoic India with the African continents.

The Ad Dawadimi terrane comprises a thick sedimentary unit (the Abt formation), large plutons of syenogranite and alkali-feldspar granite, and minor layered gabbro, ophiolite, and serpentinite mélange. The Ar Rayn terrane comprises a continental-margin volcanic arc containing volcanic, volcaniclastic, and minor sedimentary rocks (Al Amar group), locally strongly metamorphosed, voluminous calk-alkaline TTG plutonic rocks, and a significant amount of granite. The two terranes are in contact along the serpentinite-decorated Al Amar fault, which is interpreted as a suture.

The Abt formation is entirely sedimentary, but because no base is observed it is treated as a terrane in its own right, not a post-amalgamation basin like other basins described in this review. The formation is exposed over an area of about 225 km N–S and 100 km E–W sandwiched between the Afif and Ar Rayn terranes but, on the basis of its subdued magnetic signature, is inferred to continue at least 300 km to the north beneath Phanerozoic cover (Fig. 17) (Johnson and Stewart, 1995). The formation is not directly dated but a maximum depositional age of ~620–615 Ma is provided by the U–Pb age of the youngest detrital zircon retrieved from five samples of the Abt Formation (618 ± 16 Ma; Cox et al., 2011) and the youngest age (621 ± 3 Ma) of detrital zircon cores reported by Kennedy et al. (2011) (Fig. 18).

The detrital zircons, overall, are Neoproterozoic with a major cluster of ages between 710 and 600 Ma, compatible with derivation, for example, from adjacent parts of the Ar Rayn or Afif terranes. Older zircons with near concordant Mesoproterozoic ages between 1805 Ma and 2120 Ma and early Paleoproterozoic ages form a minor, but significant component of the detrital grains (Cox et al., 2011). In addition, the Nd isotopes of the Abt formation yield Mesoproterozoic model ages, demonstrating that a significant amount of pre-Neoproterozoic material makes up the protolith of these rocks. On the basis of these observations, Cox et al. (2011) suggest that the Abt Formation was derived from the adjacent composite Afif terrane as this is the only terrane in the Saudi Arabian part of the Arabian Shield to contain pre-Neoproterozoic rocks.

$^{40}Ar/^{39}Ar$ plateau ages of metamorphic muscovite in the Abt formation (618 ± 6 Ma and 621 ± 4 Ma; using the constants of Renne et al., 2010) are evidence of Abt-basin metamorphism and deformation, presumably related to basin closure (Table 1) (Cox et al., 2011). Less precise hornblende $^{40}Ar/^{39}Ar$ ages between about ~616 and 601 Ma reported by Lewis (2009), Al-Saleh and Boyle (2001) and Al-Saleh et al. (1998) from the Abt formation, the At Tari window east of the Halaban ophiolite at the western margin of the Ad Dawadimi terrane, and the Ar Ridaniyah ophiolite mélange in the north-central part of the terrane are interpreted as metamorphic and cooling ages during further exhumation. Rims on detrital zircon cores in the Abt formation yield U–Pb SHRIMP ages between ~610 and 602 Ma (Kennedy et al., 2011), which probably reflect a later hydrothermal event. Following folding and metamorphism, the formation was intruded by undeformed syenogranite and alkali-feldspar granite dated with U–Pb SHRIMP zircon ages between 579 ± 3 Ma and 565 ± 2 Ma (Kennedy et al., 2005).

The Abt formation (Abt schist) is a monotonous assemblage of well-bedded fine- to medium-grained wacke, siltstone and shale. Bedding is mostly on the scale of a few centimeters to a few meters and sedimentary structures include cross bedding and grading. Delfour (1982) suggested that the formation is a sequence of turbidites but no rigorous sedimentological study of the formation has been published, and the tectonic setting of the formation is not clear. The formation has undergone greenschist-facies metamorphism, with mineral assemblages dominated by muscovite, chlorite, and variable amounts of quartz and feldspar. The formation is folded about north-trending folds. Folds are mostly open and upright, but become tighter in the east toward the Al Amar fault. Fold limbs are characterized by at least two generations of crenulations and crenulation cleavage. The crenulations are mutually co-axial and co-axial with the regional mesoscale folding but can be identified because the youngest crenulation affects the earlier cleavage and bedding (Lewis, 2009). In the Ar Ridaniyah area, in the central part of the Ad Dawadimi terrane, typical Abt formation rocks are structurally underlain by a volcanosedimentary sequence named the Ar Ridaniyah formation. The stratigraphic/depositional relationship between the Ar Ridaniyah and Abt formations is uncertain because they are in the footwall and hanging wall, respectively, of a west-vergent thrust. Al-Saleh and Boyle (2001) interpret the volcanosedimentary rocks as part of an ophiolitic mélange, probably part of the oceanic crust on which the formation was deposited whereas Elsass (1981) and Al-Shanti and Mitchell (1976) interpret the Ar Ridaniyah formation as a basal shelf facies that passes eastward and up-section into deep water facies of the typical Abt formation. Another ophiolitic complex is present at Jabal Tays, in the southern part of the basin (Al-Shanti and Gass, 1983). On Th/Sc vs. Cr and a Th/Sc vs. Zr/Sc diagrams, the Abt formation plots in the forearc and oceanic island-arc to continental-arc fields (Lewis, 2009).

The Al Amar arc (>690–615 Ma) is the main component of the Ar Rayn terrane. It consists of tholeiitic to calc-alkaline basaltic to rhyolitic volcanic and volcaniclastic rocks with subordinate tuffaceous sedimentary rocks and carbonates (Doebrich et al., 2007). They are variably deformed and metamorphosed and, in the eastern part of the terrane, crop out as amphibolite-facies paragneiss and schist. Metallogenetically, the terrane is distinctive as the host of epithermal gold, porphyry copper, and iron oxide-copper–gold occurrences (Doebrich et al., 2007). The Al Amar group is not dated, but some of the volcanic rocks in the arc have a minimum age of 689 ± 10 Ma, based on dates from trondhjemitic intrusions (Doebrich et al., 2007). The arc contains two TTG-suites comprising a low-Al suite (Group 1) (632–616 Ma; Stacey et al., 1984; Doebrich et al., 2007) and a high-Al or adakitic suite (Group 2) (689–617 Ma; Stacey et al., 1984; Doebrich et al., 2007). Both suites plot in the field of volcanic-arc granites (Doebrich et al., 2007) and are comagmatic with the volcanic rocks. A more evolved and younger phase of magmatism is represented by late- to post-tectonic alkali-feldspar granites (Group 3). They have strongly fractionated REE patterns with strongly negative Eu anomalies and Rb and Th peaks and plot on the Y–Nb diagram of Pearce et al. (1984) in the volcanic-arc granite/syn-collisional granite fields (Doebrich et al., 2007). Group-3 plutonic rocks are dated by the SHRIMP method at 607 ± 6 Ma and 583 ± 8 Ma (Doebrich et al., 2007) and by the Rb–Sr method at 581 ± 6 Ma (Abdel-Monem et al., 1982). Overall, the rocks of the Ar Rayn terrane range from >689 Ma (the minimum age for supracrustal rocks of the arc) to about 580 Ma. Subduction-related arc magmatism terminated about 615 Ma, the minimum age of TTG intrusions, making the arc the youngest in the ANS. Group 3 alkali-feldspar granites are interpreted as post-subduction intrusions.

The Al Amar arc has an Sr- and Nd-isotopic signature suggesting a mantle source that was less depleted than the sources of the juvenile oceanic terranes in the western shield, or a mixture of more depleted mantle with continental material (Stoeser and Frost, 2006). Its geology, structure, and metallogeny are characteristic of a continental-margin assemblage (Doebrich et al., 2007). The tectonic setting of the Ad Dawadimi terrane is less certain. Nonetheless, the parallelism of the Ad Dawadimi and Ar Rayn terranes indicated by the aeromagnetic data (Fig. 17) suggests that the two acted as a coherent tectonic unit during final assembly of the ANS. Whether the Abt formation is a forearc with respect to the Al Amar arc or a back arc is not established. Doebrich et al. (2007) interpret the Abt formation as deposited above a subduction zone dipping west beneath the Afif terrane. This model is supported by Cox et al. (2011) who link the provenance of the Abt formation to the Afif terrane. Al-Saleh and Boyle (2001) interpret the formation as deposited in a backarc between the Afif and Al Amar arc caused by easterly roll-back on a west-dipping subduction zone. Stacey et al. (1984) and Al-Husseini (2000), on the other hand, model easterly subduction, treating both the Abt formation and Al Amar arc as the leading edge of a crustal block beneath central Arabia separate from the rest of the ANS—the leading edge of the Rayn microplate of Al-Husseini (2000).

Pending further study in the area, it is inferred the Ad Dawadimi and Ar Rayn terranes were in contact and had jointly sutured with the Afif and other western terranes of the ANS by the time of emplacement of the alkali-feldspar-rich granites that intrude the two terranes. Those in the Ar Rayn terrane are somewhat older (~607–583 Ma) and those in the Abt formation younger (~579–565 Ma), but both sets of granites are undeformed and intrude already folded and metamorphosed rocks of the Al Amar group and Abt formation. They provide a minimum age for deformation in the easternmost part of the Arabian Shield and imply that terrane amalgamation and suturing had ceased by about 607 Ma.

7. Late Cryogenian–Ediacaran structure

Different parts of the ANS display different structural fabrics (Fig. 19), with northerly trends dominant in the south and northwesterly trends dominant in the north. This geographic difference divides the ANS into southern and northern sections (Fig. 2) and is comparable to the differences in distribution of post-amalgamation basins and late- to posttectonic granitoids noted above. The difference is also consistent with radiometric ages north and south of the Cryogenian Bi'r Umq–Tharwah–Nakasib–Ariab suture, which separates mostly older (>750 Ma) Cryogenian basement in the south from mostly younger Cryogenian basement in the north (<750 Ma). As commented above, the distributions of post-amalgamation basins and granitoids could reflect differences in recent levels of erosion. However, because structural orientation was fixed during the Neoproterozoic deformation and is independent of erosion, a fundamental crustal difference in the ANS may be a factor in addition to recent erosional differences, applying to structure as well as post-amalgamation basins and granitoids.

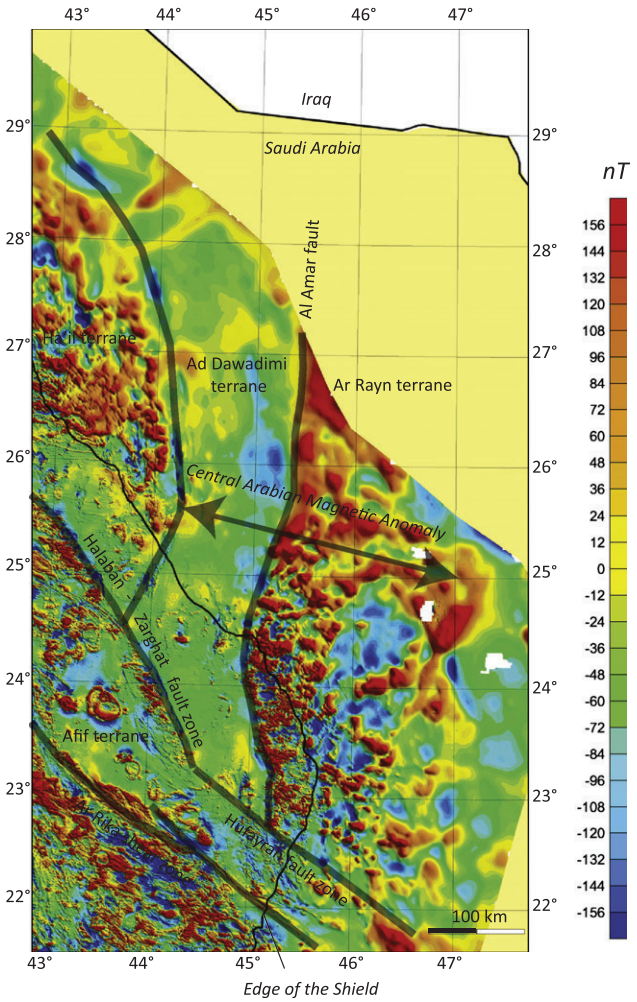

Fig. 17. Aeromagnetic-anomaly map (reduced to the pole) of central Saudi Arabia (after Zahran et al. (2003)) illustrating the continuation of the Ad Dawadimi and Ar Rayn terranes more than 300 km north of the edge of the Arabian Shield; their termination to the south at the Halaban-Zarghat and Hufayrah fault zones; and their discordant relationship with other, previously amalgamated terranes in the ANS to the west. The combined magnetic low of the Ad Dawadimi terrane and magnetic high of the Ar Rayn terrane constitutes the Central Arabian Magnetic Anomaly (CAMA) (Johnson and Stewart, 1995; Stern and Johnson, 2010). The CAMA is correlated with a fundamental crustal boundary (suture?) that extends north across the Arabian Plate to the Bitlis Zone. The magnetic data are strong evidence that the Ad Dawadimi and Ar Rayn terranes are structurally linked and, by implication, that deposition of the Abt formation is genetically associated with the Al Amar arc rather than with terranes to the west.

Some of the principal late Cryogenian–Ediacaran shear zones and shortening zones are shown in Fig. 20. Late Cryogenian–Ediacaran shearing resulted in the reactivation or dislocation of earlier suture zones, the development of new faults, and the development of suture zones in the far west (Keraf suture) and far east (Al Amar fault). Shortening is expressed by folding that is more intense than in adjacent regions and in the refolding of earlier structures such as thrusts and sutures (Abdelsalam and Stern, 1996).

7.1. High-strain zones in the southern ANS

These structures, as much as 300 km long and 1–50 km wide, comprise north-trending brittle–ductile shear zones and belts of shearing and folding (shortening zones). In the Asir and Tokar terranes and the ANS in Ethiopia, the shear zones are mostly conformable with the dominant N–S trend of bedding and fold axes, and divide the terranes into discrete structural blocks (Greenwood et al., 1982; Abdelsalam and Stern, 1996; Tadesse, 1996; de Wall et al., 2001). Some are serpentinite decorated and possibly originated during the early to middle Cryogenian as sutures between crustal units within the Asir and Tokar composite terranes, but were reactivated during the late Cryogenian to Ediacaran contemporaneously with the final convergence of eastern and western Gondwana and long after peak orogeny in the Asir terrane (680–649 Ma). One of the high-strain zones, the Keraf shear zone, is the middle-late Cryogenian (~650–580 Ma) suture at the contact between the ANS and the Saharan Metacraton (Abdelsalam et al., 1998). Others, lacking serpentinite, are strike-slip shear zones of uncertain significance. Shortening zones, where recognized in the Nubian Shield, are orthogonal to the Nakasib and Sol Hamid suture zones and associated structures (Abdelsalam and Stern, 1996). They reflect a component of localized strong E–W compression expressed by north-trending folds superimposed on earlier, mainly easterly-trending folds and thrusts (Abdelsalam and Stern, 1996; de Wall et al., 2001).

The *Nabitah fault zone* (technically a brittle–ductile shear zone, but the term "fault zone" is established in the literature) is a north-trending zone of brittle–ductile anastomosing shears in the eastern part of the Asir terrane. It extends about 430 km from the Ruwah fault zone to the Yemen border and gives its name to the 680–640 Ma Nabitah orogeny and to the Nabitah orogenic (or mobile) belt (Stoeser and Camp, 1985; Stoeser and Stacey, 1988). The fault zone originated during the Nabitah orogeny (680–640 Ma) as a phase of ductile shearing associated with the emplacement of syntectonic, mylonitic orthogneiss (Stoeser and Stacey, 1988). It was subsequently reactivated following the peak of the Nabitah orogeny and the emplacement of ~640 Ma granites (Johnson et al., 2001) as a brittle–ductile shear zone associated with offsets of limestone beds and granite contacts, normal as well as strike-slip faulting, and folding and shearing of late Cryogenian sedimentary rocks in small basins along the fault zone (Al Junaynah group, <640 Ma: Table 2). The Nabitah fault zone is interpreted as a suture

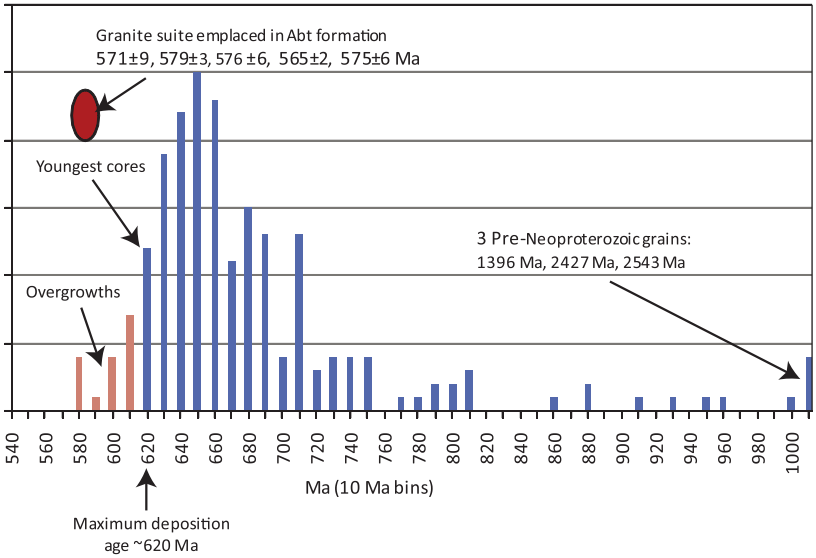

Fig. 18. Frequency plot of SHRIMP ages (±10% discordant) of zircons from the Abt formation. The youngest detrital grains with distinct cores suggest a maximum deposition age of about 620 Ma. Younger overgrowths possibly reflect hydrothermal events associated with metamorphism and later granite magmatism. The large grouping of grains dating 700–620 Ma is consistent with derivation from the Ar Rayn or other terranes to the west. Older ages indicate Tonian and Mesoproterozoic sources for some of the detrital grains, although the location of these sources is unknown. (Data from Kennedy et al. (2005, 2011), Lewis (2009) and Cox et al. (2011).)

in the north, where it separates greenschist-facies volcanosedimentary rocks of the Asir terrane from amphibolite-facies paragneiss and orthogneiss of the Tathlith terrane. In the south it is a ductile shear zone within the Asir terrane. The sense of shear on the fault zone is consistently dextral, indicated by abundant S–C and S–C′ fabrics, winged porphyroclasts, and flattened and rotated, sigmoidal conglomerate clasts. The unconformable contact between the Al Junaynah group and the ~640 Ma granites along the fault implies that the fault zone and granites underwent exhumation soon after emplacement of the granites and prior to deposition of the Al Junaynah sediments, followed by the resumption of dextral shearing.

The *Umm Farwah shear zone* extends about 200 km N–S across the central part of the Asir terrane. It is developed mostly in early Cryogenian volcanosedimentary and plutonic rocks and contains large lenses of serpentinite. At its northern end, it is the boundary between the Ablah group (640–615 Ma: Table 2) and arc rocks of the Asir terrane, and shearing here must be younger than 615 Ma. Umm Farwah shearing is also interpreted as the cause of crustal melting and emplacement of A-type granitoids (syenite; 617 ± 17 Ma; quartz-syenite and syenogranite; 605 ± 5 Ma) in the Ablah pluton (Moufti, 2001). If correct, these ages imply that brittle–ductile deformation occurred as late as 605 Ma, making the shear zone one of the youngest in the southern part of the Arabian Shield. The shear zone has S–C fabrics indicating both dextral and sinistral movements, and its overall sense of movement has not been determined. The shear zone is associated with moderate to strong folding in Ablah-group rocks about SSW-trending axes, which is consistent with transpressional sinistral shearing.

The *Muhayil* and *Sayayil shear zones* are curvilinear, northerly trending narrow zones of moderate to intense shearing in the southwest Asir terrane that continue to the north as the *Bidah shear zone*. The ages of the shear zones are unknown. The Bidah zone has a sinistral sense of movement. It is developed in the western part of the Asir terrane, in early Cryogenian volcanosedimentary rocks of the Bidah arc. Volesky et al. (2003) identified multiple episodes of deformation in the region. The earliest, D_1, episode is marked by E–W compression and the development of S_0/S_1 schistosity together with N-trending folds and mineral lineation. The D_2 episode was caused by transpressional deformation and resulted in the development of the brittle–ductile Bidah shear zone as a discrete structure. D_3 deformation comprises easterly trending, brittle, conjugate faults reflecting SE–NW shortening. D_2 and D_3 shearing postdated the early Cryogenian arc rocks of the Bidah area and sulfide mineralization (Volesky et al., 2003). The minimum age of shearing is determined by plutons of relatively undeformed biotite monzogranite and syenite and trondhjemite that intrude the sheared rocks. One of these plutons (muscovite-biotite granite) yields an Rb–Sr mineral age of 635 Ma (feldspar) (Aldrich, 1978), but it is unknown whether this is a crystallization or a metamorphic age. In summary, a lot of geochronologic work, both U–Pb zircon and Ar–Ar on hornblende and mica, is needed to resolve the ages of the N–S structures in the southern Arabian Shield.

Late Cryogenian–Ediacaran shear zones in *Eritrea* are exemplified by N-trending dextral strike-slip faults and low-angle mylonitic ductile shear zones that have both top-to-the-east and to-the-west senses of displacement (Ghebreab et al., 2005). The mylonites underwent progressive syn-deformation metamorphism at 593 ± 5 Ma (conventional U–Pb geochronology on monazite; Andersson et al., 2000) at peak *P–T* conditions of about 12 kbar and 650 °C, and have $^{40}Ar/^{39}Ar$ cooling ages for metamorphic hornblende and white mica of 579 ± 6 Ma and 567 ± 5 Ma, respectively (Ghebreab et al., 2005). The *P–T* and geochronologic data are evidence that the ductile shear zones in this part of the ANS are not merely an expression of N–S displacement associated with Ediacaran northward tectonic escape but also reflect E–W extension associated with orogenic collapse and exhumation of crustal rocks from depths of as much as 45 km (Ghebreab et al., 2005). N-trending shear zones in *southern Ethiopia* also contain a significant component of low-angle oblique normal slip manifesting regional gravitation tectonic collapse and extension, leading Tsige and Abdelsalam (2005) to conclude that N-trending belts in the southern part of the ANS are not necessarily the roots of northward expulsion of the ANS from the Mozambique Belt but are rather the expression of gravitational collapse involving detachment along low-angle shear zones.

In NE Sudan, the *Oko shortening zone* deforms rocks in the Gebeit terrane and warps the Nakasib suture, and the *Hamisana shortening zone*, the effective boundary betweeen the Gebeit and Gabgaba terranes, warps the Sol Hamid–Allaqi–Heiani suture and deforms

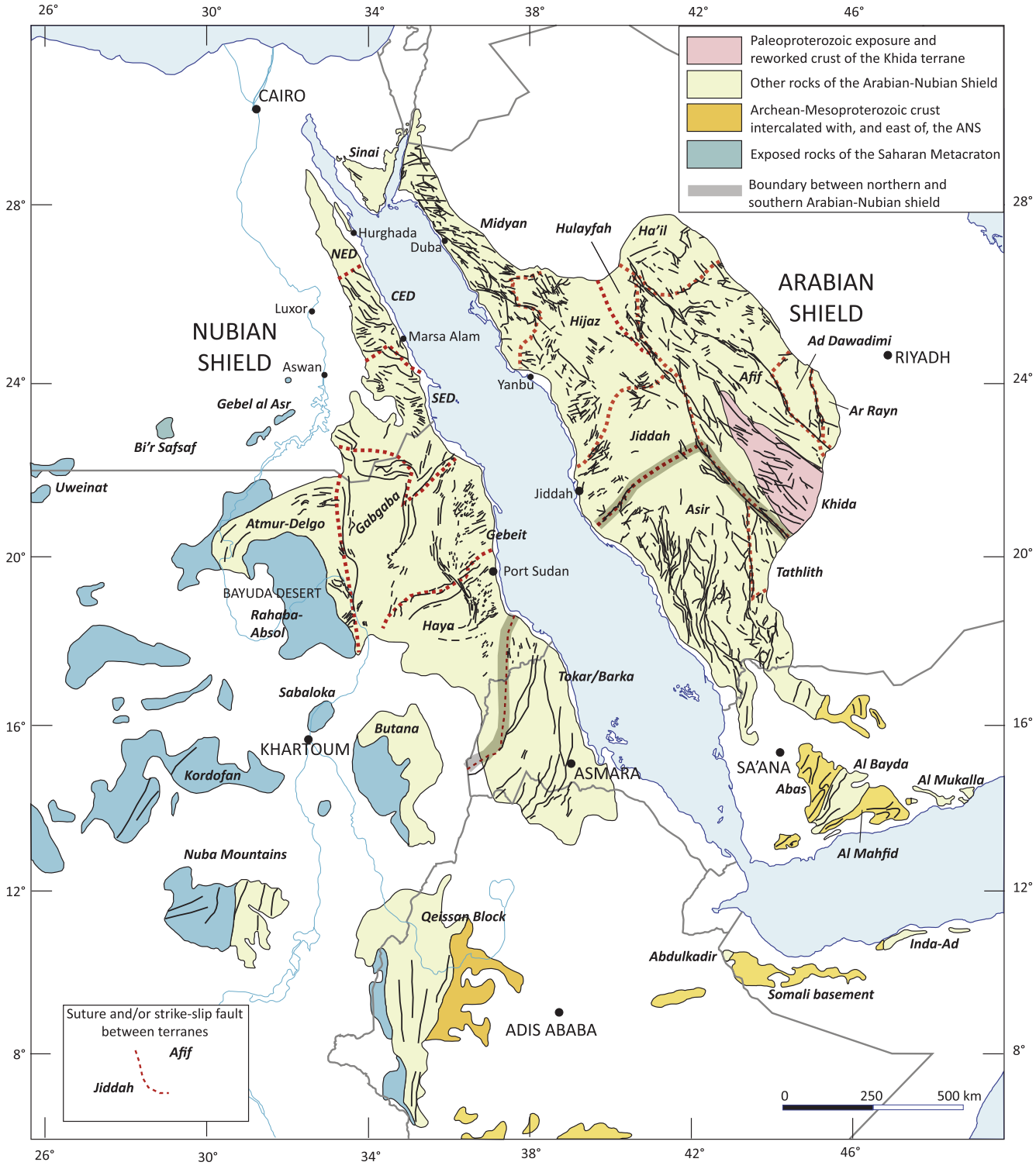

Fig. 19. Structural trends (shear zones and prominent foliation strikes) in the Arabian–Nubian Shield plotted on a base map showing the principal tectonostratigraphic terranes and suture zones (see Fig. 5B for the names and ages of the suture zones).

rocks in adjacent parts of the Gebeit and Gabgaba terranes. As noted above, the Hamisana shortening zone may continue into the Arabian Shield as the Hanabiq shear zone (Duncan et al., 1990). The shortening zones are chiefly zones of high strain that resulted in tight N–S folding rather than shearing, although a certain amount of horizontal shearing is displayed by both. Both zones are broadly sinuous and extend 200–250 km on strike and as much as 50 km across strike (Abdelsalam, 1994; Abdelsalam and Stern, 1996; Kusky and Ramadan, 2002). The Hamisana shortening zone has been variously interpreted as a suture zone, a regional shear zone, and a large-scale transpressional wrench fault. Magnetic anisotropy as well as field studies led de Wall et al. (2001) to conclude that deformation was dominated by pure shear but with a strong component of N–S extension consistent with earlier conclusions by Stern et al. (1989) and Miller and Dixon (1992). Extension was followed by minor NE–SW-trending dextral strike-slip. Thermal and tectonic activity on the zone is poorly constrained as having occurred ~660–550 Ma (Stern et al., 1989) and the zone is

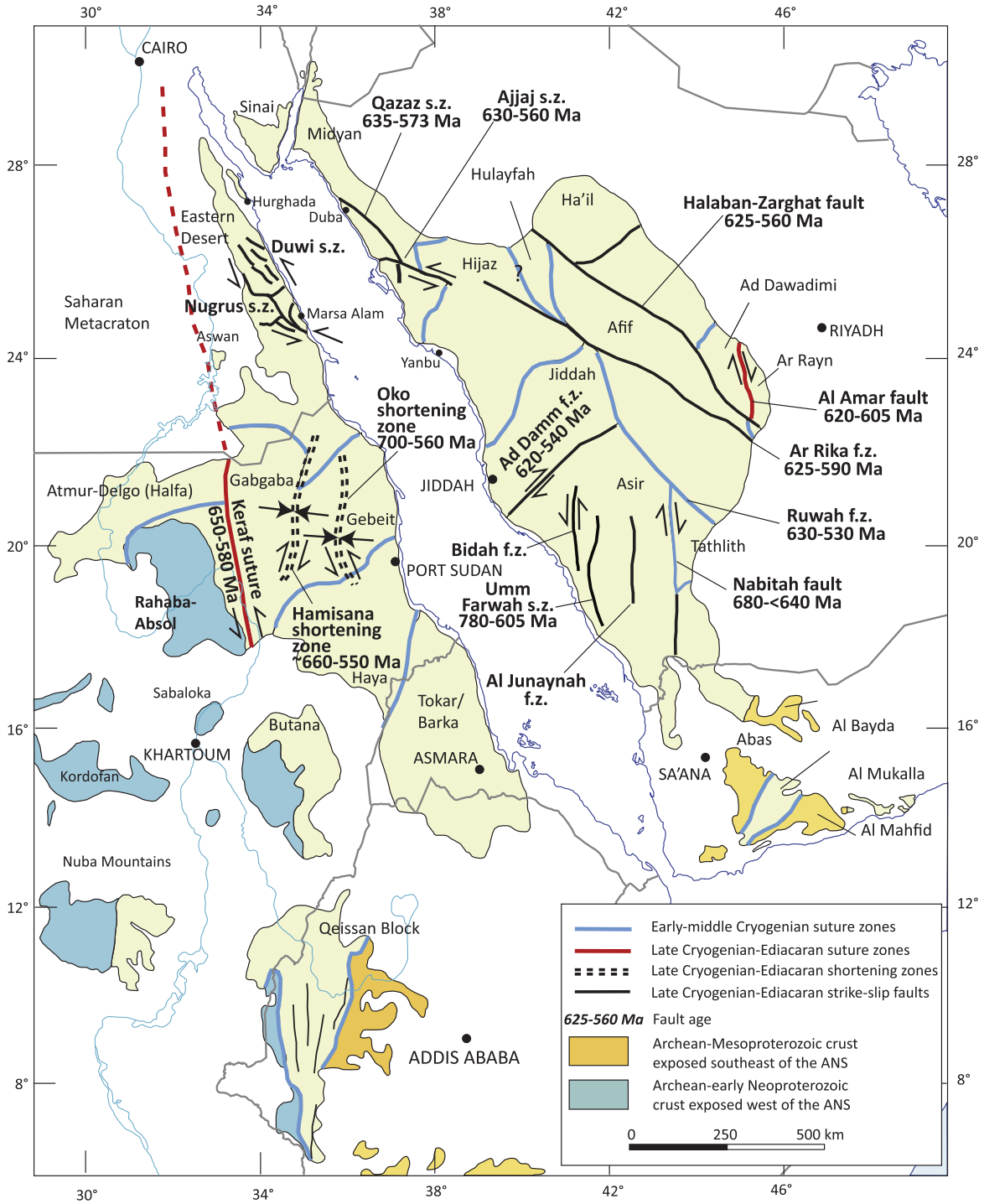

Fig. 20. ANS late Cryogenian–Ediacaran shear zones, shortening zones, and sutures.

interpreted to indicate significant middle Cryogenian–Ediacaran E–W compression.

The Oko shortening zone sinistrally offsets the 780–750 Ma Nakasib suture. It developed as an early phase of E–W compression resulting in NNW-trending tight upright folds and a later phase of subvertical NW-trending sinistral strike-slip faulting (Abdelsalam, 1994; Abdelsalam and Stern, 1996). Deformation is poorly constrained between 700 and 560 Ma.

The *Keraf suture* was broadly contemporary with the Hamisana and Oko shortening zones but has a fundamentally different tectonic significance. Rather than deforming preexisting arc assemblages and sutures, it is a major suture in its own right, comparable in age to the Al Amar suture in the Arabian Shield described below. The suture is ~500 km long and is up to 50 km wide but, as indicated in Fig. 5B, has a putative strike extension of more than 1000 km to the north, as an arc–continent suture at the border between reworked older crust of the Saharan Metacraton and juvenile crust of the ANS. Where exposed, the suture is superimposed on E- and NE-trending structures in adjacent parts of the Bayuda Desert and the Gabgaba and Atmur–Delgo terranes (Abdelsalam et al., 1998). In the north, the suture is dominated by N-trending upright folds; in the south by N- and NNW-trending sinistral strike-slip faults. The suture is interpreted to be caused by sinistral transpression along the western margin of the ANS, which

caused E–W compression as well as sinistral strike slip. The suture reflects closure of the Mozambique Ocean on the western margin of the ANS as already amalgamated terranes of the ANS converged and collided with the Saharan Metacraton. It is inferred that the suture began to develop during early oblique collision between ~650 and 600 Ma and underwent terminal collision at ~580 Ma (Abdelsalam et al., 1998). Hornblende and biotite separated from strongly deformed granite within one of the sinistral shear zones yield $^{40}Ar/^{39}Ar$ cooling ages of 577 ± 2 Ma and 577 ± 5 Ma (Abdelsalam et al., 1998). These ages are compatible with indications of orogenic activity obtained from K/Ar ages of 660 Ma for hornblende from granitoids and 560 Ma for biotite from high-grade gneiss and plutons (Bailo et al., 2003). The $^{40}Ar/^{39}Ar$ ages are evidence of very rapid cooling and exhumation following terminal collision and the cessation of ductile deformation.

7.2. Shear zones in the far eastern ANS

The Al Amar fault is a high-angle N-trending shear zone between the Ad Dawadimi and Ar Rayn terranes. It contains narrow lenses of ophiolites and carbonate-altered ultramafic rock (listwaenite and fuchsite-talc schist) (Al-Shanti and Mitchell, 1976; Nawab, 1979). The fault transects volcanosedimentary and associated plutonic rocks of the Al Amar arc (689–583 Ma), sedimentary rocks of the Abt formation ($\gtrsim$ 620 Ma), and sedimentary and volcanic rocks (Hamir group) (615–605 Ma) present in small deformed basins along the fault zone. The trajectory of convergence is unknown apart from limited observations of S–C shear fabric that suggest a component of dextral horizontal slip along the fault. The fault zone is conventionally interpreted as a suture between the Ar Rayn and Ad Dawadimi terrane, with the ultramafic rocks along the fault zone being remnants of ophiolitic crust. The timing of suturing is constrained by the observations that the Abt formation and Al Amar arc had already been deformed and metamorphosed at about 620 Ma and been uplifted at ~616 Ma prior to the emplacement of the 607–565 Ma posttectonic granites that intrude the two terranes. We therefore infer that suturing occurred between ~620–605 Ma, making the Al Amar fault the youngest suture in the Arabian Shield, broadly contemporary with the Keraf suture. As discussed in the following section, the Al Amar fault was also contemporary with the youngest movements on the Najd fault system.

7.3. Najd fault system

As originally defined (Brown and Jackson, 1960; Delfour, 1970), the Najd fault system consists of northwest-trending brittle–ductile shears in a zone as much as 300 km wide and over 1100 km long extending across the northern part of the Arabian Shield. The shears offset or reactivate middle to late Cryogenian sutures, offset Cryogenian volcanosedimentary and plutonic terrane-forming arc rocks, displace late Cryogenian–Ediacaran post-amalgamation basins, and transect late Cryogenian–Ediacaran intrusions. They are spatially associated with down-faulted blocks of the Jibalah group, gneiss domes, and gneiss belts (Fig. 10). The fault system is reported to have ~240 km cumulative displacement (Brown, 1972) but displacements of only tens of kilometers can be demonstrated for particular faults in the field. The fault zone continues NW into what, prior to Red-Sea spreading, were adjacent parts of the Nubian Shield, and is inferred, on the basis of magnetic and gravity data and paleogeographic reconstructions, to extend SE across the concealed basement of the Arabian Plate into parts of India and the Lut block of Iran that were adjacent to Arabia as Gondwanan components at the end of the Precambrian (Al-Husseini, 2000). Inferences that the Najd system extends into eastern Arabia are contested by Stern and Johnson (2010). Late Cryogenian–Ediacaran Najd-type northwest-trending transcurrent faults are present in the southern ANS and in the Mozambique Belt in Kenya and Madagascar (Raharimahefa and Kusky, 2010) and are inferred in the basement of southern Jordan, disrupted by much younger Cenozoic slip on the Dead Sea Transform (El-Rabaa et al., 2001). This extent of the fault system, if correct, would make the Najd fault system one of the largest shear systems known on Earth. Individual structures within the Najd system are brittle to brittle–ductile shears a few meters to several kilometers wide. The shears range from single, linear faults to broader sets of anastomosing shears. Movement was predominantly sinistral, although the offset of some plutons and inferences about the origin of some Jibalah group pull-apart basins suggest local dextral slip (Cole and Hedge, 1986; Agar, 1987; Matsah and Kusky, 2001; Kusky and Matsah, 2003). The shears chiefly trend NW to NNW, but a small number of NE-trending dextral shears such as the Ad Damm fault zone (Fig. 10) are believed to be conjugate shears for the Najd system (Davies, 1984).

Important features of the Najd faults include (1) transitions along strike from greenschist- to amphibolite-facies metamorphism and from brittle to ductile deformation; (2) the presence of belts and antiforms of mylonitic gneiss and schist with higher metamorphic grades than surrounding rocks; (3) the ubiquitous presence, in the high-grade rocks, of gently NW- and SE-plunging mineral and stretching lineations; (4) marker-bed offsets and microkinematic structures (S–C fabrics and rotated, winged porphyroclasts) indicating dominantly sinistral strike-slip displacement; (5) indications of local dextral strike slip during brittle faulting; (6) a juxtaposition, along some faults, of mylonitic gneiss domes, thrusts with a vergence orthogonal to the shear-zone strike, and fault-parallel and fault-oblique dikes; (7) the presence of fault-bounded basins filled by sedimentary and volcanic rocks of the Jibalah Group that either served as syn-fault, pull-apart depocenters or are younger extensional fault basins in which remnants of the Jibalah Group are preserved, or both; and (8) suspect syntectonic granitoids that form some of the orthogneisses along the fault zones (suspect because the fabric studies necessary to prove their structural setting have not yet been done). It is evident that Najd faulting involved a large component of oblique transpressional strike-slip shear, with constriction across and extension along the fault zones and vertical displacement of the sides of the fault zones relative to each other. The variations in metamorphic grade along strike indicate profound changes in P/T conditions at greenschist/amphibolite-grade interfaces of the type that are well known elsewhere to have implications for gold mineralization. The presence of suspect syntectonic intrusions (Table 3) indicates that the fault zones were favorable loci for intrusion and possibly involved feedback between intrusion and shearing. Intrusion would have thermally and hydrothermally weakened the crust; shearing would have opened up passage-ways for intrusion. An unknown structural element concerns the geometry of the Najd faults at depth. They may continue deep in the lithosphere, bottoming in horizontal detachments as envisaged by Lemiszki and Brown (1988), or flattening into listric faults. In the Arabian shield, the Najd faults have a strong magnetic and gravity expression (Fig. 21) (Mogren et al., 2008), in part reflecting an abundance of deep mafic intrusions along the faults (Gettings et al., 1986). The Najd faults are commonly modeled as a coherent structure, with an emphasis placed on features shared by individual faults, so that they are explained by a single regional cause (e.g., Moore, 1979). It should be recognized nonetheless that individual faults have distinctive structural and chronologic features (Table 3) indicating unique fault histories (Johnson and Kattan, 1999), and that the tendency to group all northwest-trending ANS faults as members of a common fault system may cause an oversimplification of interpretation of their origins.

Following interpretations by Tapponnier and Molnar (1976) and Molnar and Tapponnier (1977) for strike-slip faulting north of the Himalayas as a result of Eurasian collision with India, the Najd fault system was explained by Fleck et al. (1979) in terms of "indentor tectonics", with collision between the rocks in the Arabian Shield and a rigid block to the east. Stern (1985) pointed out discrepancies between an indentor model and the known orientations and slip directions of Najd faults, and alternatively proposed a significant role for extension in the northernmost ANS. Burke and Sengör (1986) introduced the concept of "tectonic escape" of continental material toward an oceanic free-face during collisional orogeny involving slip on transcurrent faults. In the ANS, the Najd faults are mostly modeled as transpressional structures that originated during late Cryogenian–Ediacaran oblique collision between eastern and western Gondwana, resulting in N-directed orogenic extension and escape of crust toward the paleo-Tethys ocean (Stern, 1994; Kusky and Matsah, 2003). A similar model of tectonic escape has been recently advocated for faulting in southern Africa (Jacobs and Thomas, 2004). Alternatively, the Najd system is interpreted as originating during Ediacaran–Cambrian extension associated with collapse of the East African Orogen and rifting of the Gondwana margin (e.g., Al-Husseini, 2000). A problem with the latter model is that Najd faults in the Arabian Shield predate deposition of lower Paleozoic sandstone that unconformably overlies the shield, implying that fault movement ceased by about 535 Ma, the age of the basal deposits as inferred by the youngest age of detrital zircons in the sandstone (Kolodner et al., 2006).

The principal throughgoing Najd-type structure in the Arabian Shield is the *Qazaz–Ar Rika shear zone*. It is an *en-echelon* set of shear zones that extends from the Qazaz–Ajjaj shear zone in the northwest to the Ar Rika shear zone in the southeast (Fig. 10). The Qazaz–Ajjaj shear zone hosts the Hamadat gneiss belt described above, the Ar Rika shear zone, and the Kirsh gneiss belt. Initial movements on the Ar Rika fault followed deposition of the Murdama group (~650–625 Ma) and subsequent movements followed emplacement of 611 Ma granitoids (Table 3). Gneiss and pegmatite in the Al Hawriyah antiform in the southeastern part of the Ar Rika fault zone have SHRIMP U–Pb ages indicating zircon growth at 623 Ma, 602 Ma, and 589 Ma, and possible metamorphism about 600 Ma (Kennedy et al., 2005, 2011). These results are consistent with slip on the Ar Rika fault zone between about 625 and 590 Ma. Movements on the Qazaz–Ajjaj shear zone are constrained to between ~635 and ~573 Ma (Calvez et al., 1984; Kennedy et al., 2010), bracketed by a cataclastically deformed granite with an inferred reset Rb–Sr age of 630 ± 19 Ma and the emplacement of an undeformed, post-shearing lamprophyre dike at 573 Ma that cuts paragneiss and schist along the shear zone.

The *Halaban-Zarghat fault zone* is a shorter Najd fault structure in the northern Arabian Shield. The Halaban part of the fault originated about 680 Ma as the suture at the eastern margin of the Afif composite terrane, but its trajectory deflected to the northwest during later strike-slip deformation, and the structure extended across the shield as the composite Halaban-Zarghat fault zone. Movement on the fault is predominantly sinistral and followed deposition of the Murdama group (Cole and Hedge, 1986), but subordinate dextral slip occurred after emplacement of Ediacaran diorite at 621 Ma. Along part of the fault, movement had ceased by the time of deposition of the Jurdhawiyah group (~595 Ma; Kennedy et al., 2004, 2005), but elsewhere the fault was active during and after deposition of the Jibalah group (~590–560 Ma) (Kusky and Matsah, 2003; Nettle, 2009).

As described above, the *Ruwah fault zone* is characterized by mylonitic orthogneiss, paragneiss, schist, and serpentinite of the Hajizah–Tin gneiss belt. The fault zone originated as part of the Hulayfah–Ad Dafinah–Ruwah suture zone at the western/southwestern margin of the Afif terrane, but was reactivated by Najd faulting. In the southeast, it is overthrust, along its northeastern margin, by Bani Ghayy group marble, in a region where brittle extensional fractures along the fault zone control gold-bearing quartz veins. To the northwest the Ruwah fault zone swings north and transitions into the Ad Dafinah and Hulayfah faults. The maximum age of deformation, the age of suturing, is constrained by a granodiorite gneiss protolith age of 683 ± 9 Ma (Stacey and Agar, 1985). Reactivation as a Najd fault followed deposition of the Bani Ghayy group (~650–620 Ma). Brittle–ductile deformation and metamorphism had ceased by the time of emplacement of undeformed "Najd" granite at 592 ± 4 Ma (Stoeser and Stacey, 1988; U–Pb zircon age from hornblende-biotite monzogranite).

The *Ad Damm fault zone* is a well developed NE-trending dextral strike-slip shear zone between the Jiddah and Asir terranes. It deforms the Numan complex—a granite of inferred Ediacaran age—creating mylonitic granite gneiss with very prominent rotated feldspar porphyroclasts. Fleck and Hadley (1982) suggest an age of approximately 620 Ma for the granite, which implies <620 Ma movement on the fault. Because of this age, Davies (1984) treats the fault as a conjugate dextral shear zone in the Najd system.

Although details are debated, it is widely accepted (e.g., Stern, 1985; Sultan et al., 1988) that the Najd fault system continues into the Egyptian Eastern Desert as the "Najd corridor" in the vicinity of the Hafafit, Sibai, and Meatiq gneiss domes (Fig. 16). El Ramly et al. (1990) challenged the correlation of the Najd faults across the Red Sea, arguing that claims of large-scale Najd strike-slip displacements on the margins of the Hafafit dome are not supported by the field evidence. The dispute partly reflects uncertainty as to the origin of the Meatiq and Hafatit gneiss domes. As mentioned above, some authors treat these domes as the product of exhumation associated with Najd faulting and extension, whereas others interpret the gneisses to be parts of pre-Najd thrust sheets that underwent subsequent folding or doming and were overprinted by Najd-style faulting.

The dominant shear zones around the Hafafit dome include the *Nugrus* and *Wadi Gemal thrusts* (El Ramly et al., 1984). The Nugrus thrust is a low-angle E- and N-dipping shear zone that wraps around the eastern and northern margins of the dome or is a low-angle extensional shear zone folded over the dome (Fowler and Osman, 2009). It has also been interpreted to form the base of a thrust duplex of low-grade supracrustal rocks transported to the northwest over high-grade infracrustal rocks (Greiling, 1997). The extent to which the Nugrus and Wadi Gemal thrusts were subsequently overprinted by Najd faulting is debated. El Ramly et al. (1984) and Greiling (1997), for example, show no NNW-trending strike-slip faults on their maps of the Hafafit dome. Fritz et al. (1996) infer sinistral strike-slip along the high-strain zone represented by the eastern part of the Nugrus thrust, as if the thrust was reworked by Najd strike-slip movements. Shalaby et al. (2006) show a system of linked thrusts and strike-slip faults extending from the Hafafit to the Meatiq Dome (illustrated in Fig. 16). Subsequent mapping of the northwestern end of the Nugrus shear (Fowler and Osman, 2009) however shows no further continuation of the Nugrus shear along a NW trend into the Central Eastern Desert.

The structural framework suggested by Shalaby et al. (2006) is an attractive interpretation for some Central Eastern Desert molasse basins as pull-apart basins formed at releasing bends in the shear system, accommodating orogen-parallel extension on the flanks of structural highs. There is doubt, however, about the extent of Najd faulting around the Meatiq Dome. As described above, all authors agree that the Meatiq Dome is a system of thrust stacks resulting from NW-directed tectonic translation that placed low-grade infracrustal rocks over high-grade supracrustal gneiss (Fritz et al., 1996; Loizenbauer et al., 2001; Andresen et al., 2010); but subsequent events are not agreed upon. Fritz et al. (1996, p. 311)

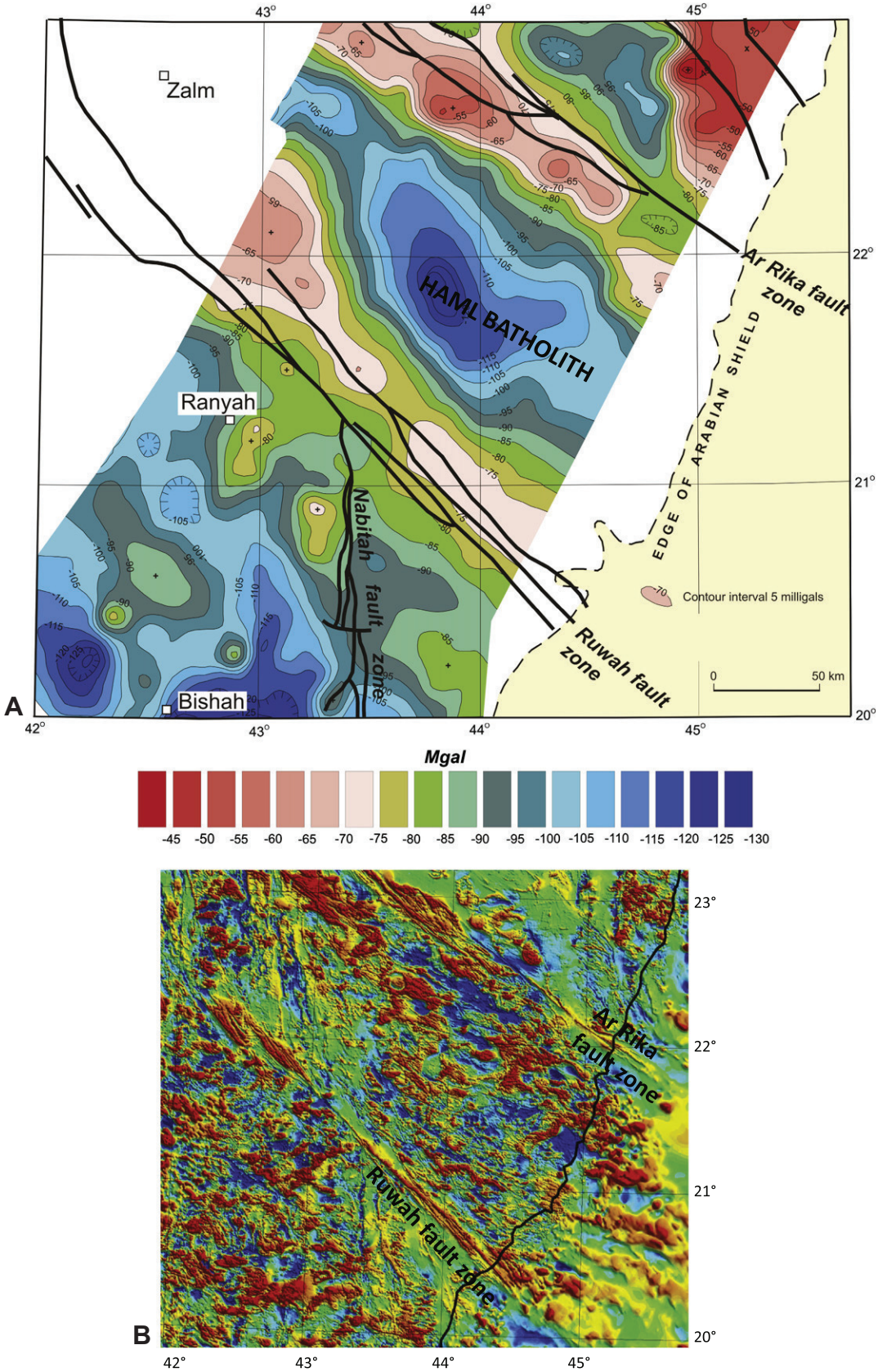

Fig. 21. Bouguer gravity (A) and aeromagnetic-anomaly maps (RTP) (B) of the eastern part of the Arabian Shield, showing the potential-field expression of Najd faults. Yellow dots on the magnetic-anomaly map are gold occurrences. The magnetic-anomaly map uses a conventional color scheme grading from red for high magnetic values through yellow and green, to blue for low values. Gravity data after Gettings et al. (1986); magnetic data after Zahran et al. (2003).

envisage that the dome was exhumed because of its setting within a "crustal-scale wrench corridor of the Najd fault system" interpreting steeply dipping, northwest-trending, high-strain zones on the east and west margins of the dome as sinistral Najd faults. Andresen et al. (2010), conversely, do not identify the bordering high-strain zones as Najd faults but interpret them as parts of the main EDSZ thrust between the infracrust and supracrust that dip steeply toward the east and west, respectively, because of folding about a NW-trending axis. This hypothesis was advanced earlier to explain the change from sinistral to dextral apparent senses on slip on the northeast and southwest flanks of a smaller gneissic culmination in the Um Had area to the west of Meatiq (Fowler and Osman, 2001).

7.4. Structural synthesis

It is well established that the ANS is part of an accretionary orogen, but as commented by Abdeen and Greiling (2005) "there is not yet any comprehensive study on the late Pan-African deformational pattern at the scale of the orogen" (p. 465). Many structural studies have been done of individual areas (e.g., Fritz et al., 1996; Worku and Schandelmeier, 1996; Blasband et al., 1997; Abdelsalam et al., 1998, 2003; Loizenbauer et al., 2001; Fowler and El Kalioubi, 2004; Abdeen and Greiling, 2005; Tsige and Abdelsalam, 2005; Fowler et al., 2006; Abdeen et al., 2008; Ghebreab et al., 2009; Andresen et al., 2010; Abdeen and Abdelghaffar, 2011) and preliminary syntheses have been done for the Central Eastern Desert (Greiling et al., 1994) and the Arabian Shield (Genna et al., 2002). Factors that currently inhibit consensus on the structural history of the ANS are a lack of systematic structural information for the region, conflicting or not-yet-resolved different interpretations, and a lack of dating of deformation and metamorphic events.

Using the Central Eastern Desert as an example of issues involved in making a structural synthesis, it is noted that the region consists of upper amphibolite-facies quartz-rich and quartzofeldspathic paragneisses and granitoid gneisses structurally overlain by (1) low-grade metamorphosed units of ophiolitic mélange (serpentinites, metagabbro, and metabasalt), island-arc mafic to felsic metavolcanics, calc-alkaline intrusive rocks, and metasediments; and (2) units of molasse (Hammamat Group) and calc-alkaline mafic to felsic volcanic rocks (Dokhan Volcanics). The high-grade rocks (variably referred to as Tier 1 and infrastructure) occupy the cores of dome-like structures. The lower-grade rocks (variously referred to as Tier 2, Pan-African nappe complex; ophiolitc nappes; and eugeoclinal rocks/eugeoclinal allochthon) form the flanks of the gneiss domes. High-strain mylonitic zones tens to hundreds of meters thick separate the high-grade and low-grade rocks and similar mylonitic zones occur within the high-grade rocks. This high-strain zone always seems to separate the high- and low-grade rocks, and it has been named the Eastern Desert Shear Zone (EDSZ) (Andresen et al., 2009, 2010). However, whether the shear zone extends as a continuous high-strain zone throughout the region or whether there are many shear zones of limited extent is not known. As commented above, despite earlier initial conclusions that the high-grade rocks are remnants of pre-Neoproterozoic continental crust (e.g., Habib et al., 1985; El-Gaby et al., 1988, 1990), the absence of significant geochemical, geochronologic, or isotopic differences between the high- and low-grade rocks strongly supports the view that they are correlative and all Neoproterozoic, belonging to the juvenile Neoproterozoic ANS crust.

The late Cryogenian–Ediacaran structural history of the CED is provisionally outlined in Fig. 22. The history illustrated extends from the end of the main collisional orogeny in the ANS, represented in the Nubian Shield by collision between the South Eastern Desert and Gabgaba terranes along the Allaqi-Heiana suture zone at 800–700 Ma (Abdeen and Abdelghaffar, 2011) and in the Arabian Shield by the Nabitah orogeny (680–640 Ma), to extension and exhumation of the ANS toward the end of the Neoproterzoic. Fowler and Osman (2001) describe bedding (S_0), gneissosity (S_g), and complex mesoscopic folds (F_g) in the high-grade rocks exposed in the core of the gneiss dome in Wadi Um Had and refer to the high-grade (garnet, cordierite, sillimanite) metamorphic event as M1. These structures and M1 metamorphism likely reflect the main collisional orogeny, and therefore date to about 700–640 Ma. S_g foliations bear a sillimanite lineation L_g. High-grade rocks in the core of the Meatiq Dome underwent a comparable early metamorphic event (referred to as M1) with peak temperatures exceeding 800 °C followed by M2 amphibolite-facies metamorphism ($T > 640$ °C, with P 6–8.5 kbar) that produced garnet-bearing assemblages (Neumayr et al., 1996a,b). It is important to note that all other, later structures (foliations, folds, lineations, thrusts, and transcurrent faults) affected the Hammamat Group and Dokhan Volcanics as well as the high-grade gneisses and low-grade eugeoclinal rocks. This imparts a common structural style to the entire region and means that, apart from the cryptic pre-640 Ma deformational event evidenced by the F_g folds in the high-grade rocks, the region has a common post-Hammamat and Dokhan structural history.

Following high-grade metamorphism, the region began to undergo orogenic collapse and extension resulting in subsidence and the development of basins that became the site of deposition of the Dokhan Volcanics and Hammamat Group (Abdeen and Greiling, 2005). Abdeen and Greiling (2005), and the authors cited by them in Table 1 in their paper (p. 460), infer general NW–SE to NNW–SSE extension. This must have occurred sometime between about 640 Ma and 630 Ma, prior to the onset of Dokhan/Hammamat deposition. Dokhan Volcanic extrusion continued until about 592 Ma and Hammamat Group deposition until 579 Ma, overlapping with subsequent deformation events and the emplacement of late- to posttectonic granites and dike swarms.

The earliest post-Hammamat structures (about or prior to 605 Ma) recognized throughout the region, reflect NNW–SSE to NW–SE shortening or northwestward gravitational collapse. Evidence for this comprises generalized ENE–WSW strikes and broad E–W-trending fold axes in several Hammamat Group basins (Abdeen and Greiling, 2005) and top-to-the-NW shearing in and around gneiss domes (Fowler and El Kalioubi, 2004). The Hammamat Group in the Hammamat basin shows an early phase of NW-directed low-angle thrusting associated with S- and SE-dipping cleavage and SE-plunging stretching lineations. Similar shortening is evidenced in other basins in the Central Eastern Desert (see Table 1 in Abdeen and Greiling, 2005). Thrusting resulted in the development of the EDSZ and its characteristic S_1 shear foliation in the Meatiq gneiss dome (Andresen et al., 2009, 2010) and the Um Had dome (Fowler and Osman, 2001). It is associated with rare F_1 folds that have axial planes parallel to S_1 (Fowler and Osman, 2001). The NW-direction of tectonic transport is evidenced by rare S–C structures, foliation"fish", shear-segmented veins (Fowler and El Kalioubi, 2004), and the intersection of S, C, and C′ surfaces (Andresen et al., 2010). In the Um Had domes, the thrust-related mylonitic fabric is associated with retrograde metamorphism (M2) of the earlier M1 metamorphic assemblages and the development of biotite-chlorite-mica schist (Fowler and Osman, 2001). The Um Had dome has a mineral-extension lineation (L_1) plunging gently NW and SE (Fig. 22) (Fowler and Osman, 2001); a similar lineation pattern is evident in the Meatiq Dome (Andresen et al., 2010). The timing of ductile deformation, and by implication the timing of the main period of NW-directed thrusting throughout the Central Eastern Desert, is constrained by the Abu Ziran syntectonic diorite (ID-TIMS age of 606 ± 1 Ma; Andresen et al., 2009).

There followed a period of NW-directed transpression associated with bulk E–W to ENE–WSW shortening. The effect of this was to develop NW–SE-trending F_2 folds, SW- and NE-dipping

thrusts, and northwest-trending transcurrent faults. In places these structures appear to be coeval as in the Wadi Queih Hammamat Group basin (Abdeen and Greiling, 2005); in other locations, such as between the Meatiq and Um Had Domes, folding and thrusting preceded transcurrent faulting (Fowler and Osman, 2001). F_2 folding is seen in the folding of the F_1 high-strain zones and S_1 foliations. The folding caused the broad girdles shown by the plots of poles-to-foliation in the Um Had area (Fig. 22), and created broad antiformal structures composed of curved outcrops of the EDSZ around the margins of the Meatiq and Um Had gneiss domes. In the Um Had area, west of the Meatiq Dome, the EDSZ is folded about a NW-trending and plunging axis (Fowler and Osman, 2001). The high-grade gneissic rocks are in the core of the antiform, creating the Um Had gneiss domes. The eastern flank of the dome is steeply dipping and here the EDSZ resembles a NW-trending sinistral transcurrent fault zone. On the western flank, the EDSZ resembles a dextral shear zone. Importantly, the folded EDSZ can be traced from the eastern to the western flanks around the northern tip of the dome, demonstrating that the margins indeed comprise a fold in the EDSZ (Fowler and Osman, 2001). A similar structure is described for the Meatiq Dome (Andresen et al., 2010), where EDSZ can be traced around the southern margin of the dome. In both cases, the eastern and western margins of the domes consist of mylonitic zones resembling transcurrent shears. As noted above, the shears flanking the Meatiq Dome have been interpreted as sinistral Najd faults, with the dome being confined to a "Najd corridor" (Fritz et al., 1996), but the observations of Fowler and Osman (2001) and Andresen et al. (2010) indicate that, what look like transcurrent shears, are the result of folding of the EDSZ.

The same bulk E–W shortening also caused the development of a zone of W- to SW-directed thrust imbrication in eugeoclinal island-arc rocks and the Dokhan Volcanics and Hammamat Group between the Meatiq Dome and the Um Had Dome (Fritz et al., 1996; Fowler and El Kalioubi, 2004). NE-dipping thrusts place the Dokhan Volcanics over the Hammamat Group, and ophiolitic mélange over the Dokhan. Duplex structures are present, and S–C fabrics confirm the sense of displacement (Greiling et al., 1996). The eastern margin of the Hammamat basin has NE-dipping thrusts that were overprinted by NNW-directed sinistral strike-slip shearing (Fowler and Osman, 2001; Abd El-Wahed, 2009). Elsewhere, SW-dipping thrusts are exposed, placing serpentinite over metagabbro and slicing and re-stacking the Hammamat Group (Fowler and Osman, 2001). Bulk shortening caused the development of NE-directed thrusts and northwest-trending folds in the Wadi Queih Hammamat basin (Abdeen and Greiling, 2005).

The concurrent, or final effect of this transpressive phase of deformation, was the production of NW-trending sinistral transcurrent faults that overprint the earlier formed SW- and NE-dipping thrusts. These faults are developed throughout the CED and, as is widely accepted, are the northwest tip of the Najd fault system. In the Wadi Queih basin these faults are associated with sub-parallel high-angle reverse faults that form a positive (half) flower structure (Abdeen et al., 1992; Abdeen and Warr, 1998) The El Mayah basin is aligned along an E–W shear belt to the south of the El Sibai gneiss dome that turns, on its western end, into a NW direction. Steep sediments are aligned and sheared along this E–W-trending structure, and the structure itself has been interpreted as a fault/shear zone conjugate to the overall NW-trending strike-slip structures (Shalaby et al., 2005, 2006). The ages of individual structures that belong to this transpressional phase of deformation are not certain, but in general it would appear that they developed by 590 Ma. Evidence for this is that thrusting in the Hammamat Group rocks in the Um Had area had occurred by the time of emplacement of the posttectonic Um Had granite (596 ± 2 Ma) and deformation in the Meatiq Dome had ceased by the time of emplacement of the Arieki granite (590 ± 3 Ma; Andresen et al., 2009). A similar constraint is provided by intrusion of leucogranites with Rb–Sr ages of 594 ± 12 and 610 ± 20 Ma (Moghazi et al., 2004) into the Nugrus shear zone on the northeast flank of the Hafafit dome. Terminal events in the CED include N–S to NW–SE extension evidenced by the dike swarms that intruded the region between about 600 Ma and 565 Ma (see Section 9.1.1), and $^{40}Ar/^{39}Ar$ ages that defined a period of peak cooling and exhumation (see Section 9.2.2. and Fig. 25).

8. Late Cryogenian–Ediacaran mineralization

Late Cryogenian–Ediacaran mineralization in the ANS is dominated by gold, the refractory metals tantalum, niobium, and tungsten (Ta, Nb, W), rare earth elements (including Y), uranium, and tin. The gold occurrences typically developed between about 650 Ma and 615 Ma (Table 4). They consist of gold-bearing quartz-carbonate veins that are commonly associated with late- to posttectonic calc-alkaline diorite, granodiorite, or granite intrusions emplaced following the Nabitah orogeny (680–650 Ma). Because the refractory metals, rare earth elements, uranium and tin are commonly (although not exclusively) associated with specialized posttectonic A-type granites, their development is clearly a result of the widespread emplacement of posttectonic A-type magmas in the ANS from about 610 Ma. Other, less common late Cryogenian–Ediacaran mineralization includes silver in quartz-carbonate veins; chromite, nickel, PGM, and ilmenite in layered mafic–ultramafic plutons; and polymetallic gold-silver-zinc epithermal mineralization together with an unusual type of zinc sulfide mineralization in the Ar Rayn terrane. It should be notes that a number of well-known metallic mineral deposits and mines in the ANS, including some that are being currently developed or explored, are outside the time-frame of this review because they are hosted by early-middle Cryogenian island-arc rocks. Such deposits include VMS Cu–Zn–Au occurrences at Jabal Say'id in the Arabian Shield and Bisha in the Nubian Shield.

8.1. Gold-quartz-carbonate veins

Gold-bearing quartz-carbonate veins have been the explored and mined in the ANS for over 6000 years (Klemm et al., 2001; Amer et al., 2009; Gabr et al., 2010). They crop out at hundreds of ancient mine sites and are worked at some of the gold mines operating in the region (Fig. 23). The veins, a type of mineralization referred to nowadays as "orogenic gold" (Groves et al., 1998; Goldfarb et al., 2001), are concentrated in areas of transpressional shearing, strike-slip faulting, and thrusting. They are preferentially concentrated in the margins and adjacent wall rocks of plutons of intermediate compositions such as diorite, tonalite, and granodiorite. A major concentration is along the Nabitah mobile (orogenic) belt in the Arabian Shield (Stoeser and Stacey, 1988). Other occurrences are adjacent to shear zones and gneiss domes in the CED of Egypt (e.g., Gabr et al., 2010; Amer et al., 2010; Greiling and Rashwan, 1994) (Fig. 23), in sheared rocks south of the Allaqi suture zone (e.g., Kusky and Ramadan, 2002) and elsewhere in the Gabgaba terrane, in transpressive shear zones in the Asmara block, Eritrea (Ghebreab et al., 2009), and in highly sheared rocks in the Tokar terrane and Queissan Block of Ethiopia. In the south Eastern Desert of Egypt, NW–SE oriented veins originated during arc–arc collision (D_1) and were subsequently deformed by D_2 folding and D_3 sinistral shearing (Abdeen et al., 2008).

Gold in these occurrences is free or associated with sulfides (arsenopyrite, chalcopyrite, sphalerite) in low-sulfide veins or disseminated in wallrock alteration zones. Gold is typically the primary economic commodity but some deposits produce

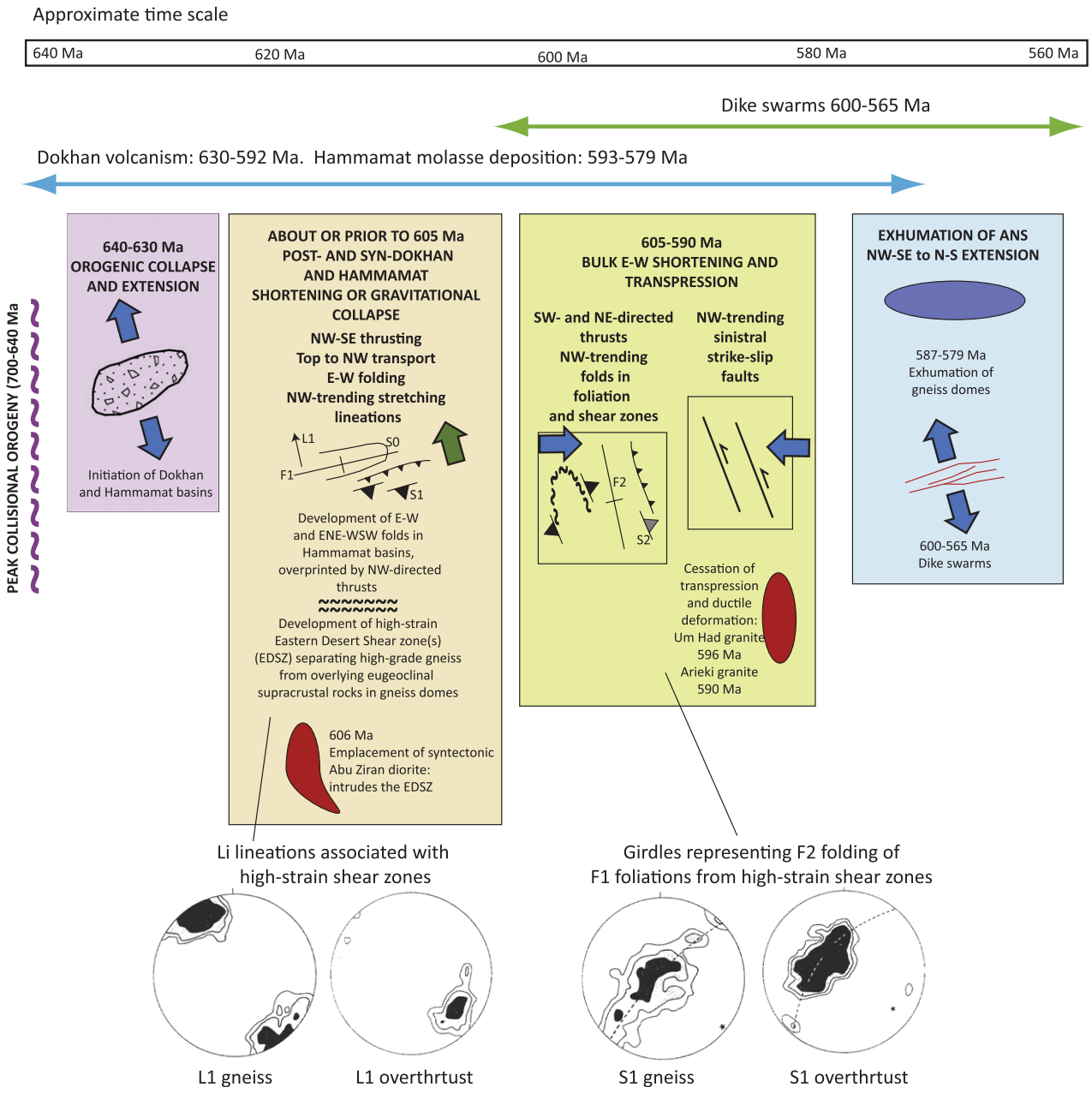

Fig. 22. Preliminary synthesis of late Cryogenian–Ediacaran structural events in the Central Eastern Desert events, largely after Abdeen and Greiling (2005), Fowler and Osman (2001), Fowler and El Kalioubi (2004), Andresen et al. (2010) and Fritz et al. (1996).

bi-product copper and zinc. Worldwide, the formation of orogenic gold reflects the passage of hot water in large volumes through permeable channel ways in a brittle structural environment or at the brittle–ductile transition at the base of the seismogenic zone (Sibson, 1987; Goldfarb et al., 2005, ref. therein). Such fluids tend to have a common composition with low salinity and high CO_2, and deposition tends to occur at a temperature of approximately 350 °C and depths of 4–12 km (Goldfarb et al., 2001).

The *Sukhaybarat–Bulghah* gold district is a large cluster of orogenic gold occurrences at the northern end of the Nabitah mobile belt in the Arabian Shield. It contains the Sukhaybarat Mine (now exhausted), the first orogenic-gold deposit developed in modern times in the ANS, which at the outset of mining in 1991 had a reserve of 17.6 t contained gold at a cutoff grade of 1.1 g/t (Al-Dabbagh and Dowd, 1996). Mineralization is hosted by sedimentary rocks of the post-amalgamation Murdama group and diorite, quartz diorite, and tonalite of the Idah suite (~620–615 Ma) (Albino et al., 1995; Al-Dabbagh and Dowd, 1996; Malmgren and Andersson, 1994). The deposit is located in a NNE-directed thrust (Malmgren and Andersson, 1994) or zone of shortening (Albino et al., 1995) at the margin of the host pluton. The veins are a few centimeters to about 1 m thick. They are low in sulfides, with arsenopyrite ± pyrite ± sphalerite ± galena ± chalcopyrite ± stibnite in the range of <1–5 wt.% (Albino et al., 1995; Lewis and Schull, 1994) and are flanked by arsenopyrite-gold-bearing alteration zones. Visible gold is not common in the Sukhaybarat–Bulghah district but individual veins at Sukhaybarat have grades of 30 g/t to as much as 200 g/t Au (Albino et al., 1995). The Sukhaybarat pluton is dated at 617 ± 2 Ma, implying that mineralization was <617 Ma (Table 4). Veins at an adjacent occurrence at An Najadi are significantly older, dated at 631 ± 12 Ma (D. Unruh, cited by Walker et al., 1994). Mineralization at the *Ad Duwayhi* prospect (31 Mt

containing 1Moz gold) (Doebrich et al., 2004), farther south along the Nabitah mobile belt, is older than Sukhaybarat. It is related to a late- to posttectonic granite (659 ± 7 Ma) and quartz porphyry (646 ± 11 Ma), and directly dated at 655.6 ± 2.7 Ma and 649 ± 2.3 Ma (Doebrich et al., 2004). The Ad Duwayhi mineralization consists of (1) gold-bearing quartz veins and breccia in and along the margins of a granite stock, and (2) a gold-bearing stockwork, sheeted quartz veins, and massive to banded quartz-rich tabular veins spatially associated with quartz porphyry.

The gold deposits of the *Nubian Shield* are more famous but less well-studied than those of Arabia. Klemm et al. (2001) concluded that Nubian gold mineralization formed when hot posttectonic granitoid plutons stimulated hydrothermal convection in the surrounding host rocks. Circulating water dissolved gold from slightly enriched mantle-derived rocks such as serpentinites and ophiolites, following joints and shear zones, altering the rocks and forming auriferous pyrite and/or arsenopyrite at 300–400 °C and 1–2 kbar. This scenario implies that most Nubian gold deposits are Ediacaran but radiometric dating is needed to test this model. The metallogenic overview presented by Botros (2002) recognizes different styles of gold mineralization at different stages in tectonic development. The island-arc stage is characterized by exhalative gold associated with BIF. The collisional-orogenic stage, just within the time-frame of this review, is associated with vein-type mineralization, the main target of gold exploration since Pharonic times, and lesser amount of gold associated with altered serpentinite (listawenite) and with the contact zones of gabbro and granite intrusions. The post-orogenic stage has small amounts of gold associated with disseminations, stockworks, and quartz veins of Sn–W–Ta–Nb.

Classic examples of vein-type, structurally controlled orogenic gold deposits in the Nubian Shield are the *Sukari mine*, 23 km SW of Marsa Alam in the Central Eastern Desert, Egypt (Arslan, 1989; Helmy et al., 2004) and the *Abu Marawat* deposit (Zoheir and Akawy, 2010). The Sukari deposit is hosted by an ophiolite and tonalitic to trondhjemitic pluton dated at 689 Ma (U–Pb ID-TIMS zircon age; Lundmark et al., 2011). The deposit is located in a NW-directed thrust duplex and is controlled by a local flower structure and extensional faults that accommodated NE–SW strike-slip deformation. Gold is present in low-sulfide (pyrite ± arsenopyrite ± sphalerite ± chalcopyrite ± galena) quartz veins and alteration zones. *P*/*T* conditions during initial vein formation were about 300 °C and 1.5–2 kbar, similar to the worldwide norms. The morphology of the veins indicates repeated veining and leaching, initiated by the intrusion of granodiorite, followed by sealing. The deposit has measured and indicated resources of 10.99 Mozs gold, inferred resources of 3.5 Mozs gold, and a reserve base of 9.1 Mozs gold (www.centamin.com.au January, 2011). The Abu Marawat deposit is interesting because it is hosted by a sequence of island-arc metavolcanic rocks and banded-iron formation. Mineralization is believed to have formed from ore fluids originating from possibly post-Hammamat granitoid intrusions leaching gold and base metals from the metavolcanics (Zoheir and Akawy, 2010). The deposit consists of sulfide-bearing quartz veins and hydrothermal breccia bodies displaying a complex history of shearing and crack-sealing quartz precipitation associated with a N-trending shear zone. Mineralization comprises pyrite–chalcopyrite ± pyrrhotite ± sphalerite ± galena. Gold is refractory in pyrite and chalcopyrite, and in rare visible gold/electrum and telluride specks.

Numerous gold-bearing quartz veins are known in western, northern and southern Ethiopia (Tadesse et al., 2003), and in several parts of Eritrea (Jelenc, 1966). In southern Ethiopia, the veins are hosted by shear zones along the contacts between low-grade volcanosedimentary rocks and high-grade gneisess. An example is the *Lega-Dembi Gold Mine* situated in the eastern boundary of the Megado zone/belt in southern Ethiopia (Ghebreab et al., 1992; Billay et al., 1997), which is currently in production. Mineralization occurred close to the peak of upper greenschist to lower-amphibolite metamorphism. Rb–Sr dating of sericite indicates an age of hydrothermal alteration and therefore of mineralization of about 545 Ma (Billay et al., 1997). This is considerably younger than gold mineralization in the main part of the ANS, and is closer to the age of orogenesis seen in the Mozambique Belt in Kenya and Madagascar—the Malagasy Orogeny of Collins and Pisarevsky (2005). Historically, hundreds of orogenic gold-bearing quartz veins were mined for gold in Eritrea, likewise in shear zones mostly within low-grade volcanosedimentary rocks (Ghebreab et al., 2009).

Table 4
Age of late Cryogenian–Ediacaran mineralization in the Arabian–Nubian shield.

Deposit name	Age of mineralization	Comment	Source
Orogenic gold			
Sukhaybarat gold	<617 Ma	Mineralization not directly dated, but must be younger than the Sukhaybarat pluton dated at 617 ± 2 Ma	Albino et al. (1995)
An Najadi gold	631 ± 12 Ma	Age of host pluton and inferred age of veining	Walker et al. (1994)
Ad Duwayhi gold	655.6 ± 12 Ma and 649 ± 2.3 Ma	Direct dating of veins; compare ages of associated plutons 659 ± 7 and 646 ± 11 Ma	Doebrich et al. (2004)
Lega-Dembi gold	545 Ma	Rb–Sr dating of sericite in hydrothermal alteration zone; constrains gold mineralization to about 545 Ma	Billay et al. (1997)
Refractory metals, Sn. W			
Kenticha tantalum	530 ± 2 Ma	Age of host pegmatite; associated with plutons dated between 550 and 520 Ma	Worku and Schandelmeier (1996) and Yibas et al. (2002)
Silsilah tin	587 ± 8 Ma	Deposit not directly dated; age inferred from that of host alkali feldspar granite	Du Bray (1984)
Ba'id al Jimalah tungsten	569 ± 16 Ma (age of granite host); ~575 Ma (age of quartz vein)	Age inferred from that of host microgranite and quartz vein	Cole and Hedge (1986) and Stacey and Stoeser (1984)
Kushaymiyah molybdenite–tungsten	<611 ± 3 Ma	Mineralization not directly dated; but must be younger than host granodiorite and quartz monzonite	Agar et al. (1992)
Ghurayyah REE	<577 ± 4 Ma	Ghurayyah stock has been dated but most zircons are about 660 Ma and probably inherited; the crystallization age of the stock is more reasonably constrained by the age of the adjacent Dabbagh pluton (577 ± 4 Ma) dated by Hedge (1984)	Hedge (1984)

8.2. Granitoid-associated refractory metals

Refractory-metals mineralization is not abundant in the ANS (Fig. 24) but, individually, some of the occurrences are of significant size and the region has the potential to become a major source of refractory metals (Küster, 2009). The host rocks are felsic intrusions, commonly referred to as "specialized granitoids" in discussions about refractory-metal mineralization in the ANS. They are chemically distinctive with K/Rb < 200, Ba < 200 ppm, Sr < 80 ppm, and Rb > 200 (Ramsay, 1986), may have peraluminous or peralkaline characteristics, and reflect extensive fractionation and geochemical evolution (Küster, 2009). The intrusions have I- and A-type affinities, and range in composition from granodiorite, monzogranite, syenogranite, to alkali-feldspar and alkali granite.

Defined by their extraordinary resistance to heat and wear, the refractory metals, strictly speaking, include niobium, molybdenum, tantalum, tungsten, and rhenium, but more generally include titanium, vanadium, chromium, zirconium, hafnium, ruthenium, osmium, and iridium. Because ANS occurrences of refractory metals commonly also include tin and(or) rare-earth elements, all these commodities are considered in this section.

In the ANS, distinctions can be recognized, depending on the composition of the host granitoids. Ta–Sn–Rb–Li–Be–Nb mineralization is mostly associated with peraluminous specialized granitoid; Nb–Zr–Y–REE–U–Th–Ta–Rb–Sn mineralization is associated with peralkaline specialized granitoids (Küster, 2009); and occurrences dominated by tin or tungsten are hosted by alkali-feldspar granite and subordinate granodiorite. The country rocks of the mineralized granitoids vary from previously deformed and metamorphosed arc terranes, to younger post-amalgamation, moderately deformed sedimentary assemblages, to serpentinite and other rocks in shear zones. The specialized granitoids themselves are posttectonic A-type intrusions. They may be strongly discordant small plutons or stocks, stocks within or on the margins of larger granitoid plutons, sheet-like bodies emplaced in tension gashes resulting from extension following the main phase of compressional deformation, or late pegmatites. As noted in a review of tin mineralization by Plimer (1987), but equally relevant to other special metals, these types of occurrences are associated with the last phase of posttectonic granites in extensional and/or shear tectonic regimes, and commonly occur in the apical parts of the intrusions.

8.2.1. Tantalum–niobium–REE–uranium mineralization

This type of mineralization is being mined at *Kenticha* in Ethiopia, is under development at *Abu Dabbab* in the Eastern Desert of Egypt, and is under exploration at *Ghurayyah*, in the Midyan terrane of northwestern Saudi Arabia.

Kenticha, in the Adola belt (south of the southern margin of Fig. 24) is a working mine with an indicated reserve ~17 Mt of ore grading 150 g/t Ta_2O_5. It is the largest known peraluminous pegmatitic rare-metal occurrence in the ANS (Küster, 2009). The deposit comprises a flat-lying, sheet-like body of peraluminous spodumene-albite pegmatite. in the midst of a 30-km long zone of pegmatites emplaced in sheared volcanosedimentary rocks, high-grade schist, and quartz-feldspar gneiss. The pegmatites and associated plutons of low-*P*, I-type biotite granite intrude a region with north-trending shears and thrusts but are posttectonic (Küster, 2009). They intruded post-collisional transtensional to extensional faults that reactivated the older structures. Plutons in the area are dated between 550 Ma and 520 Ma (Worku and Schandelmeier, 1996; Yibas et al., 2002); the Kenticha pegmatite has an emplacement age of 530 ± 2 Ma (U–Pb tantalite age; Küster et al., 2007). Other pegmatite-hosted occurrences in the ANS are at Laferug and Majayahan in Ethiopia (Küster, 2009).

Ghurayyah is hosted by a circular stock (0.9 km across) of porphyritic peralkalkaline arfvedsonite-alkali feldspar granite in the northwestern Midyan terrane (Küster, 2009). The stock is likely comagmatic with the adjacent larger Dabbagh granite, dated at 577 ± 13 Ma (Aleinikoff and Stoeser, 1988). Contacts of the stock dip steeply and wall rocks are only locally altered. Mineralization comprises disseminated columbite–tantalite, zircon, and thorite, and on the basis of limited drilling, constitutes a resource of nearly 400 Mt grading 245 g/t (0.024%) Ta_2O_5, 2840 g/t (0.28%) Nb_2O_5, 8915 g/t (0.89%) ZrO_2, and 1270 g/t (0.13%) Y_2O_3. Similar, but smaller, peralkaline-associated occurrences are at Jabal Hamra, Jabal Tawlah, Jabal Said, and Umm al Birak (Collenette and Grainger, 1994).

Abu Dabbab, in the Eastern Desert, is hosted by peraluminous granite, as is Nuweibi, and Nikrab in the Nubian Shield and Umm al Suqian in the Arabian Shield (Küster, 2009). The Abu Dabbab granitic body is a sheet- to stock-like intrusion as much as 300 m across, emplaced in early–middle Cryogenian ophiolitic mélange. The stock was probably intruded into tension gashes developed along a northwest-trending shear zone. The intrusion consists of strongly altered alkali-feldspar granite hosting disseminated Nb–Ta (columbite–tantalite) and Sn (cassiterite) minerals. Quartz and quartz–topaz veins occur in apical parts of the intrusion. The 44.5 Mt deposit is projected to produce more than 650,000 lb Ta_2O_5 per year over a mine life of 20 years as well as approximately 1530 tonnes of tin per year and may well become the world's largest supplier of tantalum feedstock (Gippsland Ltd., 2009, cited from company website February 2011 http://www.gippslandltd.com/). The Nuweibi prospect, 20 km S of Abu Dabbab, is an alkali-feldspar stock up to 2.2 km across. The stock has relatively high Ta content in its eastern part, where it contains indicated and inferred resources of 98 Mt ore grading 146 g/t Ta_2O_5 (Gippsland Ltd., 2007; cited by Küster (2009)).

A somewhat different type of mineralization consisting of U, Nb, Ta, and emerald is located along the Nugrus Shear Zone, in the Eastern Desert, Egypt. It is associated with alkaline pegmatites and granites (Lundmark et al., 2011). The mineralization is dated at 608 ± 1 Ma by ID-TIMS dating of a Nb–Ti oxide (Lundmark et al., 2011) tentatively identified as polycrase extracted from the Zabara orthogneiss. The orthogneiss has a protolith age of 633 ± 5 Ma. The Nb–Ti oxide has U contents in excess of 5% and also contains Y and Ta along with minor Ce, Th and Ca. It is proposed that the mineralization results from a hydrothermal flux associated with emplacement of highly fractionated syn- to post-kinematic leucogranites in the Nugrus Shear Zone (e.g. Abdalla and Mohamed, 1999; Lundmark et al., 2011). The leucogranites have Rb–Sr ages of 594 ± 12 and 610 ± 20 Ma (Moghazi et al., 2004), consistent with the Nb–Ti oxide age.

8.2.2. Tin and tungsten mineralization

Concentrations of tin and tungsten in the ANS are known in the northeastern Arabian Shield. The *Silsilah* tin prospect comprises low hills of greisenized granite in cupolas of an alkali-feldspar granite pluton (du Bray, 1984), surrounded by a large ring of alkali and alkali-feldspar granite (587 ± 8 Ma; Cole and Hedge, 1986) about 6 km in diameter. The mineralization is hosted by hydrothermally altered alkali-feldspar granite and comprises pods and disseminations of cassiterite in topaz–quartz and topaz–muscovite–quartz greisen. The deposit contains an estimated resource of some 1.5 Mt at an average grade of 0.19% Sn.

The *Ba'id al Jimalah* tungsten occurrence is located at a small intrusion of greisenized and quartz-veined porphyritic two-feldspar (perthitic microcline and albite) microgranite (569 ± 16 Ma; Cole and Hedge, 1986) emplaced in Murdama group sedimentary rocks about 100 km S of Silsilah. The occurrence is at the apex of an intrusion composed of interconnected and merging sills and